

The comparison of LVIS, and RIEGL LiDAR data
in a Tropical Dry Forest

by

Chenzherui Liu

A thesis submitted in partial fulfillment of the requirements for the degree of

Master of Science

Department of Earth and Atmospheric Sciences
University of Alberta

© Chenzherui Liu, 2023

Abstract

Studying structural changes in tropical forests is essential for understanding changes in ecosystem complexity. In this thesis, I studied changes in ecosystem structure using two different airborne Light Detection and Range (LiDAR) systems collected 16-years apart (the 2005 dry season and the 2022 wet season). Line- and shape-based waveform metrics were used to document structural changes in secondary Tropical Dry Forests located in Santa Rosa National Park, Guanacaste, Costa Rica.

My analysis based on a 16-year growth period showed significant variations in canopy height-related profiles, particularly in the RH50, RH100, and other waveform-produced metrics such as (Cx and Cy). Our results revealed that the centroid location on tree height (Cy) and the derived Radio of Gyration (RG) present significant changes.

Moreover, I observed positive correlations between Cy and CH, RG and RH100 especially in the wet season data collected in 2021. These findings not only enhance our understanding of the growth dynamics of TDFs in Santa Rosa National Park but also provide valuable insights that can inform future conservation efforts. By comprehending these complex chronosequence changes and growth patterns, we can develop effective strategies for preserving and managing these critical ecosystems in a changing world.

Preface

This thesis is an original work by Chenzherui Liu.

Acknowledgements

First, I would like to acknowledge my supervisor Dr. Arturo Sanchez-Azofeifa, kind heart and consistent help, not only in your academic guidance but also in the care you show. Your very first email, “welcome to join the team,” was a precious opportunity for me. This gift was not just a study position but also a steppingstone for extending my horizons and achieving my life goals. Fortunately, during the pandemic, your guidance and trust helped keep me on track. Thank you to Dr. Arturo Sanchez-Azofeifa for all your time and efforts to guide me to be a better person and encourage my academic achievement.

Secondly, I would like to thank Dr. Michael Hesketh. Your gentle and patient teaching was of great help during my first year of study. I will always remember that the first mid-term review, the guidance from you, and the trust you had in me helped me believe that I could succeed in an academic setting. Thank Dr. Michael Hesketh, without your understanding and humor, I would not have been a confident student.

I would also like to thank the CEOS family, as everyone from the laboratory was connected. I appreciate the opportunity to meet all of you and form strong bonds. You are all amazing people who have lightened my life. I am so grateful that I can meet all of you. Thank you to my friends Connor Bax, Steven Wagers, Patrick O'Brien, Mohammed Abdaki, Nooshin Mashhadi, Paula Moreno Pina, Ronny Alexander Hernandez Mora, Andre Truksa, Nelson Mattie, and my friends who have graduated: Oscar Javier Baron Ruiz, Yuhui Ke, Tao Han, Menglei Duan and Jose Guzman (names not listed in order). Your kindness, care, and positivity have meant the world for me.

Finally, I want to send my love to my parents. Thank you for your love and support in this regard. Without you, I would have had nothing. Nothing can be compared to my lovely, Mom and Dad. I Love you.

Table of Contents

1.0 INTRODUCTION	1
1.1 REFERENCES.....	8
2.0 STUDYING TROPICAL DRY FORESTS SECONDARY SUCCESSION (2005-2021) USING TWO DIFFERENT LIDAR SYSTEMS	13
2.1 ABSTRACT.....	13
2.2 INTRODUCTION.....	14
2.3 STUDY AREA.....	17
2.4 DATA AND METHODS.....	19
2.4.1 <i>LVIS data and RIEGL LMS-Q680i data</i>	19
2.5 METHODS.....	20
2.5.1 <i>Description of workflow</i>	20
2.5.2 <i>Pseudo-waveform synthesis (RIEGL to LVIS)</i>	23
2.5.2.a <i>Tree height from waveform</i>	26
2.5.2.b <i>Waveform metrics</i>	28
2.5.2.c <i>Age group and succession stages</i>	30
2.6 RESULTS.....	31
2.6.1 <i>Change in relative height traits and canopy height</i>	31
2.6.2 <i>Comparison of waveform centroid metrics</i>	36
2.6.3 <i>Comparing waveform line-shape based metrics</i>	39
2.6.4 <i>Relation between the metrics</i>	42
2.7 DISCUSSION.....	46
2.7.1 <i>Mapping forest with time series by LiDAR</i>	47
2.7.2 <i>Seasonal impact of the TDFs comparison</i>	49
2.8 CONCLUSION.....	52
2.9 REFERENCES.....	53
3.0 CONCLUSION	59
3.1 SUMMARY AND CONTRIBUTION.....	59
3.2 FUTURE WORK.....	61

3.3 REFERENCES.....	63
REFERENCES.....	65

List of Tables

Table 1: Parameters of LVIS and RIEGL LMS-Q680I LiDAR systems.....	6
Table 2 : Description of the LiDAR metrics used in this study. WAF is the waveform amplitude figure, and NCE is the normalized cumulative return energy figure. H_g is the ground return which means elevation of the lowest detected mode within the waveform (m).	22
Table 3: 2005(LVIS) and 2021(RIEGL) mean Relative Height with the 25%, 50%, 75% and 100% energy back with one standard deviation. Data is grouped as a function of successional stages.	32

List of Figures

Figure 1. Location of the Santa Rosa National Park Environmental Monitoring Super Site in Guanacaste, Costa Rica, and the footprint of the LVIS data and the RIEGL LMS-Q680i data used in this study. The color ramp in LVIS, ranging from blue to yellow, represents the elevation changes from low to high. In the RIEGL LMS-Q680i system, a color gradient from dark red to white signifies a similar shift in elevation, with low elevations represented by lighter colors and higher elevations by darker shades18

Figure 2. Workflow applied to the LVIS and RIEGL datasets to analyze changes in forest structure as a function of successional stage between 2005 and 202120

Figure 3. LVIS footprints are recorded with a footprint diameter of 20-meters for the 2005 flight. The RIEGL system used a 1-meter footprint to derive a discrete point cloud from the waveform information in 202124

Figure 4. Workflow associated with the processing of the waveforms: 1. The LVIS centroids were located. 2. The discrete point cloud is clipped using the standard LVIS radius 3. The .h5 files are derived from all of those individual point clouds. Then we compared the LVIS (2005) waveform and the.h5 waveform from RIEGL (2022).....25

Figure 5. The tree top is the first return represented by **Hb**, the main ground return is represented by **Hg**, and **Hτ** is the tree height during the wet season. During the wet season, more leaves return the energy from the tree top and waveform showing the dominant peak in the main canopy. During the wet season, more leaves return energy from the tree top and waveform, showing a dominant peak in the main canopy.27

Figure 6. The left figure represents a waveform from the dry season. During this time of year, the TDF's leaves drop substantially, the canopy returns and the energy absorption are lower than during the rainy season. The ground returns from the dominant crest of the waveforms.....27

Figure 7. Density chart showing the density of Canopy Heights (CH) in 2005 and 2021. Blue represents the LVIS 2005 and orange represents RIEGL 2021.34

Figure 8. Point graph showing the different Canopy Heights (CH) for the early, intermediate and late successional stages in 2005, and then changes to the intermediate, late1, and late2 stages in 2021. Curved circles represent the density. When circle size increases, a lower density is represented.....35

Figure 9. Point graph showing Cx and Cy as representing each footprint's centroid of the 2005 waveforms. Separated colours express the early stage in dark, intermediate stage in red and the late stage in blue.36

Figure 10. Point graph using Cx and Cy to represent each footprint's centroid of the 2021 waveform. Separated color express the intermidiate stage in dark, the late1 stage in red and the late2 stage in blue.38

Figure 11. Frequency distribution of Cx illustration changes between 2005 and 2021.....39

Figure 12. Frequency distribution of Cy illustration changes between 2005 and 2021.....40

Figure 13. Line graph illustrating the density of the RG distribution in 2005 and 2021.41

Figure 14. Point graph showing the RG points grouped by the early, intermediate and late stages. The X axis represent the LVIS 2005 data and the Y axis is RIEGL 2021 data. The color from black, red and blue represent the early stage, intermediate stage, and late stage respectively.....42

Figure 15. Correlation graph showing the relation between the Cx, Cy, RG, CH and RH100 metrics in 2005. The color gradient represents the degree of positivity or negativity between the measurements. Blue is negative, whereas red is positive.....44

Figure 16. Correlation graph showing the relation between the Cx, Cy, RG, CH and RH100 metrics in 2021. The color gradient represents the degree of positivity or negativity between the measurements. Blue is negative, whereas red is positive.....45

1.0 Introduction

A Tropical Dry Forest (TDF) is an ecosystem defined as having more than 50% of its deciduous trees growing with a mean annual temperature of ≥ 25 °C and total annual precipitation between 700 and 2000 mm (Sánchez-Azofeifa *et al.*, 2005). Approximately 54% of the total area of tropical dry forests (TDFs) is located in the Americas, encompassing an estimated 519,600 km². Specifically, Central America account for 203,900 km² or approximately 39% of the total TDF area in the Americas. (Portillo-Quintero & Sánchez-Azofeifa, 2010). TDFs are ecosystems that provide a niche for many different types of species and steadily contribute to many multifunctional ecosystem services (Sánchez-Azofeifa *et al.*, 2005; Calvo *et al.*, 2017; Poorter *et al.*, 2019). By the end of the 20th century, secondary TDFs had become the dominant land cover type in many Latin American countries as a result of a slowdown in deforestation and an increase in conservation initiatives (Castillo *et al.*, 2012).

Seasonality and the capacity to support deciduous species are two of the most readily identifiable characteristics of TDFs in the neotropical forest (Murphy, 2008). The dry season in the Central America, characterized by no rainfall, lasts from December to May of the following year (McLaren *et al.*, 2003). Prolonged dry periods are a significant feature of TDFs and shape the ecology of these ecosystems, driving patterns in vegetation structure, species composition, and ecosystem processes. As a result of this seasonal drought, 90–95% of deciduous trees shed their leaves to reduce evaporation (Jaramillo *et al.*, 2003). At the beginning of the rainy season

(June), rain replenishes TDFs with moisture, allowing for enhanced leaf production and canopy expansion (Gu *et al.*, 2018).

Over the past few decades, several studies have contributed to a better understanding of the ecological dynamics of TDFs (Sánchez-Azofeifa *et al.*, 2005; Castro *et al.*, 2010). A common denominator of these efforts is the need to map TDFs as a function of successional stage. Successional stage is defined as the regeneration of forest growth from natural or human disturbances (Kalacska *et al.*, 2004). Generally, successional stages are characterized using the vertical and horizontal structure of the forest, leaf flushing dynamics, and density of green canopy cover (Lebrija-Trejos *et al.*, 2011). TDF succession, however, is influenced by other variables such as Leaf Area Index (LAI), species composition, length of wet and dry seasons, canopy height, land-use history, soil type, and age since abandonment (Almeida *et al.*, 2019, Arroyo-Mora *et al.*, 2005). Therefore, secondary TDFs can be classified into three successional stages: early, intermediate, and late (Arroyo-Mora *et al.*, 2005).

The unique ecology of TDFs underscores the importance of studying and conserving these ecosystems, which are important for their biodiversity, ecosystem services, and human well-being. For ecological remote sensing studies, early, intermediate, and late successional stages can be mapped by comparing the aforementioned variables over time and space (Castillo *et al.*, 2012). From a chronological point of view, and considering the number of years since abandonment of a given parcel of land, early forests are those with a chronological age between 0-15 years, intermediate forests are those with ages between 15-35 years, and late forests as

those with more than 35 years (Arroyo-Mora *et al.*, 2005). Late TDFs' forest are not necessarily the climax, but they are used as a final reference based on changes in structure and composition (Calvo-Rodriguez *et al.*, 2017). In general, early TDFs deciduous trees account for 80%-100% of the total number of stems; however, in the older succession stage, the percentage of deciduous trees can drop to between 30% and 50% (Arroyo-Mora *et al.*, 2005). Over time, deciduous trees and lianas dominate TDFs, with this last structural group becoming more dominant in the intermediate stages (Falcão *et al.*, 2015). Lianas generally contribute to a reduction in canopy openness and an increase in the woody area index (Sanchez-Azofeifa *et al.*, 2017).

Light Detection and Ranging (LiDAR) has become a commonly used technology for understanding the vertical and horizontal characteristics of TDFs (Castillo-Núñez *et al.*, 2011). Unlike passive optical techniques, LiDAR systems use a self-emitted laser beam to illuminate a target and measure the beam albedo (Asner *et al.*, 2014). The differences in the beam's return times and frequency can be used to estimate the distance and shape of the target. LiDAR systems can be categorized into three types: (1) Terrestrial Laser Systems (TLS), (2) airborne systems, and (3) spaceborne systems. Ground, airborne, and spaceborne LiDAR systems deal with the quantification of forest structure differently, despite the use of the same physical principles (Almeida *et al.*, 2019). For example, ground-based LiDAR systems are advantageous for layer profiles and tree/liana structures because they record data from the bottom to the top of the forest. This property makes it possible to capture tree branch elements such as tree stems with precision and accuracy not available before, and can be compared to the bird's eye perspective obtained from airborne and spaceborne LiDAR systems (McCombs *et al.*, 2003).

On the other hand, airborne LiDAR systems (especially drone-based systems) provide a unique opportunity to characterize temporal changes in forest structure due to phenology (Sanchez-Azofeifa *et al.*, 2017). As a result, LiDAR systems (ground, airborne, and spaceborne) are among the most efficient and accurate methods available to ecologists and conservation biologists to study ecosystems (Martinuzzi *et al.*, 2013).

Many different types of airborne LiDAR systems are currently available, such as the Land, Vegetation, and Ice Sensor (LVIS) from the National Aerospace Administration (NASA), the Leica SPL100, the Galaxy from Teledyne Optech, and the RIEGL LMS-Q680I are the current airborne platforms. LiDAR data can be estimated using two approaches: discrete return (DR) and full-waveform (FW). The utilization of a small footprint and the capture of diverse reflectances from each beam in DR LiDAR systems enable the acquisition of highly precise information that is essential for extensive research, especially in the fields of aboveground biomass and individual tree studies (Sumnall *et al.*, 2016). The small footprint of the DR LiDAR system provides high-resolution data, facilitating detailed analyses of individual trees and other objects, which, in turn, enhances our understanding of forest composition and structure (Reyes-Palomeque *et al.* 2021). In addition, the DR LiDAR system captures multiple returns from a single laser pulse, enabling acquisition of more detailed information on the distribution and characteristics of the forest canopy (Fedrigo *et al.*, 2018). These highly accurate and precise data have numerous applications in forestry, ecology, and other related fields. Although DR LiDAR systems offer many advantages, they also have some limitations that need to be considered. One of the main disadvantages of DR LiDAR is that it is unable to penetrate dense vegetation, resulting in underestimation of forest canopy height and biomass (Sumnall

Hill and Hinsley, 2016). Another disadvantage of DR LiDAR is that it requires clear visibility and a line of sight between the sensor and the ground surface (Clark et al., 2011). This means that it is not suitable for use in areas with heavy cloud cover or during adverse weather conditions such as rain or snowfall.

Nonetheless, full-waveform (FW) LiDAR is a powerful technology that has gained considerable attention in recent years because of its ability to capture highly detailed information about the physical properties of vegetation and terrain. FW LiDAR systems record the entire waveform of backscattered light, providing more detailed information on the vertical distribution of vegetation and ground objects (Sumnall *et al.*, 2016). This technology has several advantages over other LiDAR systems, including improved accuracy in estimating forest biomass and greater ability to penetrate dense vegetation (Park et al., 2011). Despite its numerous advantages, the full-waveform LiDAR has some limitations. One of the main drawbacks is that they can be expensive to operate and maintain, making them less accessible to some researchers and organizations (Fieber et al., 2015). In addition, the processing of waveform data can be complex and time-consuming, requiring specialized technical expertise and computational resources.

One of the most reliable instruments, Land Vegetation and Ice Sensor, has been used to collect Earth science data for decades. The LVIS collects ground features with a 1064 nm-wavelength (Table 1) laser containing three detectors (Huang *et al.*, 2012). From its first mission in 1998, LVIS collected data from several regions, including Greenland, Alaska, Central America, and

Canada. In 2005, NASA used a King Air B-200 airplane installed with an LVIS sensor to collect data from northwest Costa Rica using a 20m footprint (Castillo *et al.*, 2011, Huang *et al.*, 2012). On the other hand, the RIEGL LMS-Q680I provides full-waveform collection through echo signals collected from the subjects on the surface (Table 1). Since 2008, the RIEGL LMS-Q680I has been regarded as one of RIEGL's most dependable devices (Park *et al.*, 2011). Data from the RIEGL LMS-Q680I, using a 1550 nm-wavelength LiDAR system, can determine variations within two millimetres based on 266 000 readings per second (Jalobeanu *et al.*, 2012). The RIEGL LMS-Q680I can properly estimate the structure and profile of a given forest using a modified flight route and a high-density cloud point. In the majority of cases, the RIEGL LMS-Q680I outperformed the TLS, particularly regarding the generation of Digital Terrain Models (DTM) (Jalobeanu *et al.*, 2012). Consequently, contemporary research on forest structure and archaeology has benefited from this sensor (Cavender-Bares *et al.*, 2020).

Table 1: Parameters of LVIS and RIEGL LMS-Q680I LiDAR systems

	Footprint size	Wavelength	accuracy	Operating altitude	Pulse firing rate	Operation date
LVIS	20m	1064nm	≤2m	<10km	100-500Hz	1995-present
RIEGL LMS-Q680I	0.5m	1550nm	≤20mm	1-1.6km	80k-240kHz	2008-present

Source: <http://www.riegl.com/nc/products/airborne-scanning> and

<https://lvis.gsfc.nasa.gov/Home/index.html>

Numerous studies have been conducted in recent years at Santa Rosa National Park (SRNP) using LiDAR systems (Sánchez-Azofeifa, *et al.*, 2015; Gu *et al.*, 2018; Zhao *et al.*, 2021). However, only a few studies have compared TDFs over a 16-year period. Dupuy *et al.*, (2012) studied the TDF in the Yucatan over a period of 60 years and found that the vegetation structure and composition of TDFs varied significantly with time since abandonment. Specifically, researchers found that forest height, basal area, and species richness increased with time since abandonment, while stem density decreased. Additionally, they found that soil nutrients, topography, and climate are important predictors of forest structure and composition. Falcão *et al.* (2015) argued that a better understanding of these strategies can help inform conservation and management efforts as well as improve our understanding of the ecological processes that drive TDF dynamics, while highlighting the importance of these traits in enabling plant species to thrive in highly variable and dynamic environments. Furthermore, Reyes-Palomeque *et al.*, (2021) presented a study on the use of LiDAR to map forest age and characterize vegetation structure and species composition in TDFs. The authors argue that LiDAR technology can be a valuable tool for mapping and monitoring TDFs, which can help inform conservation and management strategies. The study also underscores the need for further research on TDFs, particularly in the areas of forest age and succession, to better understand these important ecosystems and protect them for future generations.

Given the need to understand the different capabilities of the LVIS and RIEGL LMS-Q680i systems, this thesis aims to study changes in the structure of TDFs located at the Santa Rosa National Park Environmental Monitoring Super Site (SRNP-EMSS) over a 16 year span (2005–2021) using point cloud and waveform LiDAR data.

1.1 References

Almeida, D.R.A. et al. (2019) ‘Monitoring the structure of forest restoration plantations with a drone-lidar system’, *International Journal of Applied Earth Observation and Geoinformation*, 79(March), pp. 192–198. doi:10.1016/j.jag.2019.03.014.

Arroyo-Mora, J. P. *et al.* (2005) ‘Secondary forest detection in a neotropical dry forest landscape using Landsat 7 ETM+ and IKONOS imagery’, *Biotropica*, 37(4), pp. 497–507. doi: 10.1111/j.1744-7429.2005.00068.x.

Asner, G.P. and Mascaro, J. (2014) ‘Mapping tropical forest carbon: Calibrating plot estimates to a simple LiDAR metric’, *Remote Sensing of Environment*, 140, pp. 614–624. doi:10.1016/j.rse.2013.09.023.

Calvo-Rodriguez, S. *et al.* (2017) ‘Changes in forest structure and composition in a successional tropical dry forest’, *Revista Forestal Mesoamericana Kurú*, 14(35), p. 12. doi: 10.18845/rfmk.v14i35.3149.

Castillo-Núñez, M. *et al.* (2011) ‘Delineation of secondary succession mechanisms for tropical dry forests using LiDAR’, *Remote Sensing of Environment*, 115(9), pp. 2217–2231. doi: 10.1016/j.rse.2011.04.020.

Castillo, M. *et al.* (2012) ‘LIDAR remote sensing for secondary Tropical Dry Forest identification’, *Remote Sensing of Environment*. Elsevier Inc., 121, pp. 132–143. doi: 10.1016/j.rse.2012.01.012.

Cavender-Bares, *et al.* (2020) Remote sensing of plant biodiversity, *Remote Sensing of Plant Biodiversity*, pp. 581. doi: 10.1007/978-3-030-33157-3.

Clark, M. L. *et al.* (2011) ‘Estimation of tropical rain forest aboveground biomass with small-footprint lidar and hyperspectral sensors’, *Remote Sensing of Environment*, 115(11), pp. 2931–2942. doi: 10.1016/j.rse.2010.08.029.

Dupuy, J. M. *et al.* (2012) ‘Patterns and Correlates of Tropical Dry Forest Structure and Composition in a Highly Replicated Chronosequence in Yucatan, Mexico’, *Biotropica*, 44(2), pp. 151–162. doi: 10.1111/j.1744-7429.2011.00783.x.

Falcão, H. M. *et al.* (2015) ‘Phenotypic plasticity and ecophysiological strategies in a tropical dry forest chronosequence: A study case with *Poincianella pyramidalis*’, *Forest Ecology and Management*, 340, pp. 62–69. doi: 10.1016/j.foreco.2014.12.029.

Fedrigo, M. *et al.* (2018) ‘Predicting temperate forest stand types using only structural profiles from discrete return airborne lidar’, *ISPRS Journal of Photogrammetry and Remote Sensing*. Elsevier B.V., 136, pp. 106–119. doi: 10.1016/j.isprsjprs.2017.11.018.

Fieber, K. D. *et al.* (2015) ‘Validation of Canopy Height Profile methodology for small-footprint full-waveform airborne LiDAR data in a discontinuous canopy environment’, *ISPRS Journal of Photogrammetry and Remote Sensing*. Elsevier B.V., 104, pp. 144–157. doi: 10.1016/j.isprsjprs.2015.03.001.

Gu, C. *et al.* (2018) ‘Using LiDAR waveform metrics to describe and identify successional stages of tropical dry forests’, *International Journal of Applied Earth Observation and Geoinformation*. Elsevier, 73(January), pp. 482–492. doi: 10.1016/j.jag.2018.07.010.

Huang, W. *et al.* (2012) ‘Mapping forest above-ground biomass and its changes from LVIS waveform data’, International Geoscience and Remote Sensing Symposium (IGARSS). IEEE, pp. 6561–6564. doi: 10.1109/IGARSS.2012.6352096.

Jalobeanu, A. *et al.* (2012) The full-waveform LiDAR Riegl LMS-Q680I: From reverse engineering to sensor modeling Coastal Monitoring using UASs View project Accuracy and effectiveness of orthophotos obtained from low cost UASs video imagery for traffic accident scenes documentation View project. Available at:
<https://www.researchgate.net/publication/267556394>.

Jaramillo, V. J. *et al.* (2003) ‘Biomass, Carbon, and Nitrogen Pools in Mexican Tropical Dry Forest Landscapes’, *Ecosystems*, 6(7), pp. 609–629. doi: 10.1007/s10021-002-0195-4.

Kalacska, M. *et al.* (2004) ‘Species composition, similarity and diversity in three successional stages of a seasonally dry tropical forest’, *Forest Ecology and Management*, 200(1–3), pp. 227–247. doi: 10.1016/j.foreco.2004.07.001.

Lebrija-Trejos, E. *et al.* (2011) ‘Environmental changes during secondary succession in a tropical dry forest in Mexico’, *Journal of Tropical Ecology*, 27(5), pp. 477–489.
doi:10.1017/S0266467411000253.

Martinuzzi, S. *et al.* (2013) ‘Quantifying Tropical Dry Forest Type and Succession: Substantial Improvement with LiDAR’, *Biotropica*, 45(2), pp. 135–146. doi: 10.1111/j.1744-7429.2012.00904.x.

McCombs, J. W. *et al.* (2003) ‘Influence of fusing lidar and multispectral imagery on remotely sensed estimates of stand density and mean tree height in a managed loblolly pine plantation’, *Forest Science*, 49(3), pp. 457–466. doi: 10.1093/forestscience/49.3.457.

McLaren, K.P. *et al.* (2003) ‘The effects of moisture and shade on seed germination and seedling survival in a tropical dry forest in Jamaica’, *Forest Ecology and Management*, 183(1–3), pp. 61–75. doi:10.1016/S0378-1127(03)00100-2.

Murphy, P.G. (2008) ‘Ecology of Tropical Dry Forest Author (s): Peter G . Murphy and Ariel E . Lugo Source : Annual Review of Ecology and Systematics , Vol . 17 , (1986), pp . 67-88 Published by : Annual Reviews Stable URL : <http://www.jstor.org/stable/2096989>’, *Ecology*, 17(1986), pp. 67–88.

Park, H. J. *et al.* (2011) ‘Analysis of pine tree height estimation using full waveform lidar’, 34th International Symposium on Remote Sensing of Environment - The GEOSS Era: Towards Operational Environmental Monitoring, pp. 3–6.

Poorter, L. *et al.* (2019) ‘Wet and dry tropical forests show opposite successional pathways in wood density but converge over time’, *Nature Ecology and Evolution*. Nature Publishing Group, 3(6), pp. 928–934. doi: 10.1038/s41559-019-0882-6.

Portillo-Quintero, C. A. *et al.* (2010) ‘Extent and conservation of tropical dry forests in the Americas’, *Biological Conservation*, 143(1), pp. 144–155. doi: 10.1016/j.biocon.2009.09.020.

Reyes-Palomeque, G. *et al.* (2021) ‘Mapping forest age and characterizing vegetation structure and species composition in tropical dry forests’, *Ecological Indicators*, 120, pp. 106955. doi: 10.1016/j.ecolind.2020.106955.

Sánchez-Azofeifa, G. A. *et al.* (2015) 'Structural effects of liana presence Structural effects of liana presence in secondary tropical dry forests using ground LiDAR Structural effects of liana presence', *Biogeosciences Discuss*, 12, pp. 17153–17175. doi: 10.5194/bgd-12-17153-2015.

Sánchez-Azofeifa, G. A. *et al.* (2005) 'Research priorities for neotropical dry forests', *Biotropica*, 37(4), pp. 477–485. doi: 10.1111/j.1744-7429.2005.00066.x.

Sánchez-Azofeifa, G. A. *et al.* (2017) 'Can terrestrial laser scanners (TLSs) and hemispherical photographs predict tropical dry forest succession with liana abundance?', *Biogeosciences Copernicus GmbH*, 14(4), pp. 977–988. doi: 10.5194/bg-14-977-2017.

Sumnall, M. J. *et al.* (2016) 'Comparison of small-footprint discrete return and full waveform airborne lidar data for estimating multiple forest variables', *Remote Sensing of Environment Elsevier Inc.*, 173, pp. 214–223. doi: 10.1016/j.rse.2015.07.027.

Zhao, G. *et al.* (2021) 'Hyperspectral and Full-Waveform LiDAR Improve Mapping of Tropical Dry Forest' s Successional Stages', *Remote Sensing*, 13(19), pp. 1–27. doi:10.3390/rs13193830.

2.0 Studying Tropical Dry Forests secondary succession (2005-2021) using two different LiDAR systems

2.1 Abstract

Chronosequence changes among Tropical Dry Forests (TDFs) are essential for understanding this unique ecosystem, which is characterized by its seasonality (wet and dry) and a high diversity of deciduous trees and shrubs. From 2005 to 2021, we used two different airborne LiDAR systems to quantify structural changes in the forest at Santa Rosa National Park. Line- and shape-based waveform metrics were used to record the overall changes in the TDF structure. Based on a 16-year growth analysis, notable variations in height-related profiles were observed, particularly for the RH50, RH100, and waveform-produced canopy heights. The results showed that Cy and RG have increased since the forests have been growing, whereas Cx has decreased. The decrease in Cx is due to the fact that ground returns are less when canopy density grows and canopy height increases. A positive relationship was observed between Cy and CH, RG and RH100 especially in the wet season data collected in 2021. These findings provide important insights into the growth dynamics of TDFs in Santa Rosa National Park, and could inform future conservation efforts.

2.2 Introduction

At the beginning of the XXI century, Tropical Dry Forests (TDFs) spanned 3.4 million hectares in Central America (Marín et al., 2005). Despite the considerable extent of these forests, a significant portion remains unprotected and susceptible to unregulated deforestation and land use/cover change policies such as agricultural expansion, anthropogenic fires, and illegal logging (Marín et al., 2005). These anthropogenic forces have severely disrupted ecosystem services, including the provision of drinking water, biodiversity conservation, and climate regulation, particularly over the past two decades (Siyum, 2020). Although measures such as logging bans and the establishment of national parks have been implemented for preservation, the future dynamics of TDFs remain uncertain. The existing knowledge regarding the continuous safeguarding of TDFs and their future evolution is insufficient.

Over the past three decades, remote sensing has become increasingly important for studying ecological processes within TDFs, with both passive and active platforms being employed. Applications of these platforms have concentrated first on mapping TDFs extension and growth rates (Kennard *et al.*, 2002), and then on the characterization of their vertical structure and composition (Li et al., 2017). Currently, remote sensing studies are aimed at characterizing tropical secondary forest structure and composition (Castillo-Núñez et al., 2011). The former, presents new challenges to remote sensing (Castillo-Nez *et al.*, 2011; Martinuzzi *et al.*, 2013; and Gu, *et al.*, 2018). For example, Gillespie *et al.* (2009) used passive remote sensing to study the richness of tropical forests (dry, moist, and wet), which was later expanded in a study by Chitale *et al.*, (2019), who used the Normalized Difference Vegetation Index (NDVI) from

Landsat Thematic Mapper data from 2010 to develop a sound estimation of plant species richness and identify areas of high biodiversity. In terms of active remote sensing studies, Ghulam *et al.*, (2014) and Solberg *et al.*, (2017) have used active InSAR remote sensing data to study the invasive species and forest biomass. Among these active systems, Light Detection and Ranging (LiDAR) has shown potential in addressing some of the limitations of radar systems by providing more precise estimates of vegetation height and sensitivity to shifts in structural attributes, making it essential for distinguishing different forest successional stages, particularly in secondary forests. (Castillo *et al.*,2012).

The LiDAR technology works by measuring the intensity and travel duration of a laser pulse reflected by a canopy to create a three-dimensional map, which determines the distance between objects by measuring the travel return time of a given pulse (Park *et al.*, 2011). However, LiDAR systems face application challenges, particularly in dense tropical forests, where various canopy layers and tree branches become major laser beam reflectors. Such problems can be resolved using longer wavelength waveforms, because airborne topographic LiDAR systems use wavelengths between 905 and 1550 nm, which, in turn, balances the penetration depth of the laser signal and its absorption by water (Schneider *et al.*,2014). In secondary forests, full-waveform LiDAR systems can use reflected energy to collect additional data such as the canopy and understory profile of a given forest plot.

More specifically, the amount of time a beam of light travels is converted into a distance to distinguish between the first return, which often originates from components positioned at the

top of the canopy, and the most recent return (ground returns) (Pirotti *et al.*, 2011). The method of converting the amount of time spent traveling into distance yields a dataset that evaluates the heights of targets located significantly below the trajectory of the detector. This approach has been extensively employed in diverse climatic ecosystems to analyze forest characteristics such as canopy height, aboveground biomass, and forest structure (Stan *et al.*, 2019). As the laser signal travels through the canopy, it comes into contact with different forest structural components (e.g., branches and leaves), facilitating differentiation between secondary and primary/mature forests (Sánchez-Azofeifa *et al.*, 2015). However, the absence of forest age information in successional studies poses a significant hurdle for accurately estimating biodiversity and forest function (Castillo-Núñez *et al.*, 2011).

The process of assessing the structural successional changes in tropical secondary forest, in relation to their respective successional stages, has emerged as an indispensable and unrivaled technique for elucidating the intricacies of plant community dynamics (Janzen, 2000).

Secondary forests vary in their species composition and forest structure over time, showing trade-offs in plant architecture in line with the dynamics of the succession stage (Zhao *et al.*, 2021). LiDAR technologies enable the establishment of the relative age of a forest by observing its structure (tree height, Diameter at Breast Height (DBH), and species composition) (Phillips *et al.*, 2017). Numerous studies, such as those of Zhao *et al.* (2021), used hyperspectral, full-waveform LiDAR data and machine learning classifiers to map early, intermediate, and late successional stages. Zhao's *et al.* (2021) data fusion approach, combined with machine learning classifiers, demonstrated that LiDAR systems are an essential data source for improving the accuracy of forest age identification in TDFs.

Nevertheless, few studies have used LiDAR to study temporal changes as a function of successional stage. Considering the potential contributions of multitemporal LiDAR acquisitions to the understanding of tropical forest changes as a function of ecosystem succession, the purpose of this study was to use airborne LiDAR information collected in 2005 and 2021 to study changes in the structural attributes of a TDF. Specifically, LiDAR waveform derived metrics were used to characterize changes between early, intermediate, and late forests over a period of 16 years.

2.3 Study area

This study was conducted at Santa Rosa National Park's (SRNP) environmental monitoring super site in Guanacaste (Figure 1), northwest Costa Rica ($10^{\circ}48'53''$ N, $85^{\circ}36'54''$ W). Since 1971, the SRNP has been part of the Costa Rica National Park system and a component of the Guanacaste Conservation Area (Allen, 2001). The SRNP was originally a hacienda that slowly recuperated into a mosaic of different forest patches with different successional stages (Meléndez Chaverri, 1974).

The topography of the study area is rather flat (approximately seven percent slope), and from northwest to southeast, the elevation drops from 325 masl to sea level. The bulk of precipitation at the SRNP falls during the six-month rainy season, with an annualized rate of roughly 1,750 mm (May-November) (Sánchez-Azofeifa *et al.*, 2005). The average annual temperature of the

2.4 Data and methods

2.4.1 LVIS data and RIEGL LMS-Q680i data

In 2005, the LVIS-equipped King Air B-200 aircraft collected surface reflectance data above the SRNP. The LVIS system captured over 180,000 waveforms decoded from 432 bins for each LiDAR echo beam (Table 1). Under the LVIS Data Structure (LDS) coding, the original binary data were reorganized to LVIS Canopy Elevation (.lce), LVIS Ground Elevation (.lge), and an LVIS Geolocated Waveform (.lgw) formats respectively.

The second dataset was obtained from the RIEGL LMS-Q680i system. Using a high laser pulse (repetition rate up to 400 kHz) and more than 260,000 measurements per second, the RIEGL LMS-Q680i collects high-quality data independent of the complexity of the terrain (Table 1). In 2021, Stereo Carto Central America provided a 2000 m scan of the SRNP image with 1m resolution. After image pre-processing and raw laser processing, *.tif contained image data, and the *.las file restored point clouds data that are used in this study.

It is noticeable that the data collection by the LVIS was conducted during the dry season of 2005, a period during which most trees were in a leaf-off stage. This limited tree canopy crown density influenced the energy returned to the sensor, resulting in modifications to the waveform when compared to the leaf-on season data collected by the RIEGL LMS-Q680i. In 2021, the RIEGL LMS-Q680i gathered leaf-on data from TDFs during the wet season. During the leaf-on season, the proliferation of leaves in the TDFs resulted in a greater number of canopy returns.

2.5 Methods

2.5.1 Description of workflow

In this study, two different types of LiDAR systems were used for the analysis, as indicated above. The workflow used in this study is illustrated in Figure 2. The workflow aims to 1) upscale the small footprints from RIEGL (1m) to LVIS (20m), 2) produce the RIEGL waveform and unify its format with the LVIS data, 3) produce the tree waveforms, 4) separate three successional stages, and 5) conduct a comparison using waveform metrics between 2005 and 2021.

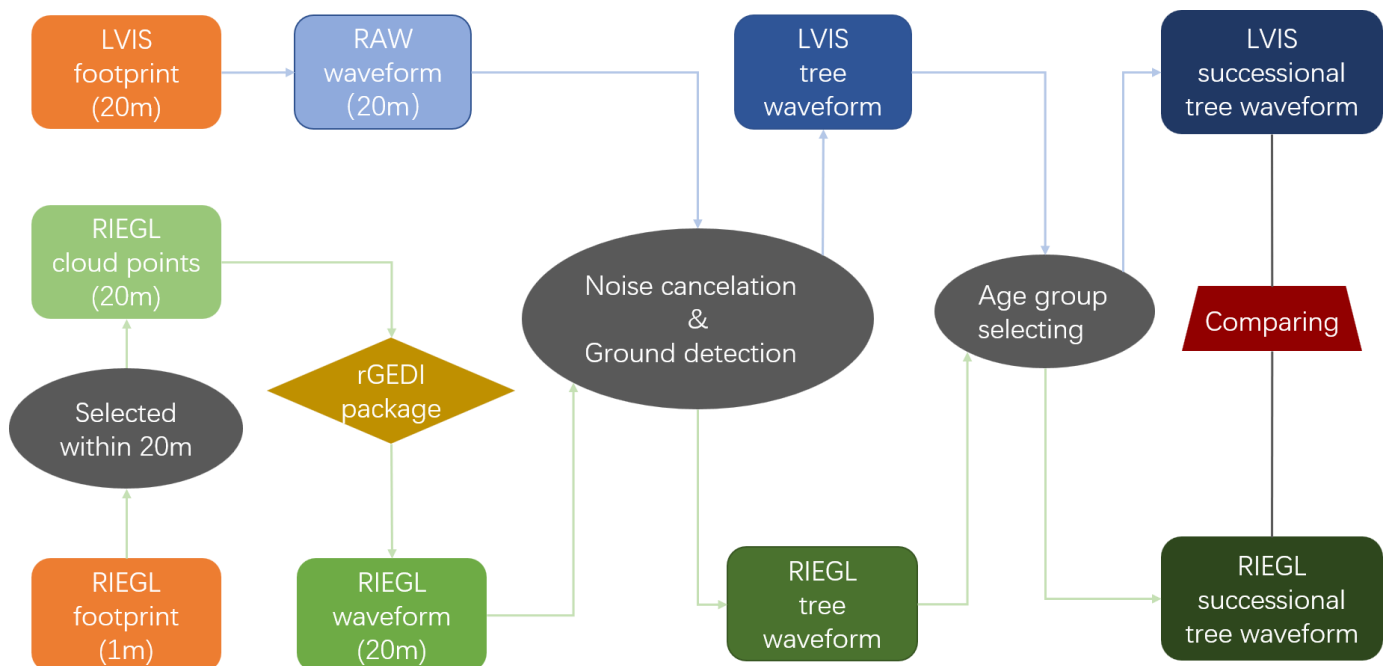


Figure 2. Workflow applied to the LVIS and RIEGL datasets to analyze changes in forest structure as a function of successional stage between 2005 and 2021.

This analysis was performed using the LVIS LiDAR 2005 and RIEGL LMS-Q680i 2021 waveforms. The following variables were extracted from the two datasets for 2005 and 2021 (Table 2): Canopy Height (CH) and Relative waveform Intensity at 25, 50, 75 and 100% of the vertical profile (RH25, RH50, RH75 and RH100), which quantified the vertical changes in vegetation; the visualized balanced point (centroid) of the waveform (C_x and C_y) (Eq:1), which depicted the changes in waveform amplitude and waveform sensitivity and the Radio of Gyration (RG), which quantified the changes in waveform shape.

Eq1:

$$C = \frac{\int f(x,y) dl}{\int dl} \quad (1)$$

Table 2 : Description of the LiDAR metrics used in this study. WAF is the waveform amplitude figure, and NCE is the normalized cumulative return energy figure. H_g is the ground return which means elevation of the lowest detected mode within the waveform (m).

Acronym	Source	Unit	Description
RH25	NCE	meter	Relative Height related to H_g at which 25% of the waveform energy occurs.
RH50	NCE	meter	Relative Height related to H_g at which 50% of the waveform energy occurs.
RH75	NCE	meter	Relative Height related to H_g at which 75% of the waveform energy occurs.
RH100	NCE	meter	Relative Height related to H_g at which 100% of the waveform energy occurs.
Cx	WAF	waveform amplitude	The x coordinate of the waveform centroid (under the waveform coordinate system)
Cy	WAF	meter	The y coordinate of the waveform centroid (under the waveform coordinate system)
RG	WAF	null	The second moment of the waveform or the radius of gyration, is the root mean square of the sum of the two-dimension distances that all points on the waveform are from its centroid (under the waveform coordinate system)

Annual rate	null	%/year	The annual rate is calculated by the increased value divided by the total years, then divided by the total increased amount. In the thesis, the time period is constant at 16 years.
-------------	------	--------	--

2.5.2 Pseudo-waveform synthesis (RIEGL to LVIS)

To compare forest changes between the two data collections, the smaller footprint (1 m) from the RIEGL system must be upscaled to match the larger footprint (20 m) of the LVIS system (Figure 3). In addition, the formats of the two LiDAR systems should be unified. Hence, several conversions were necessary to match the RIEGL (2021) dataset with the LVIS (2005) dataset.

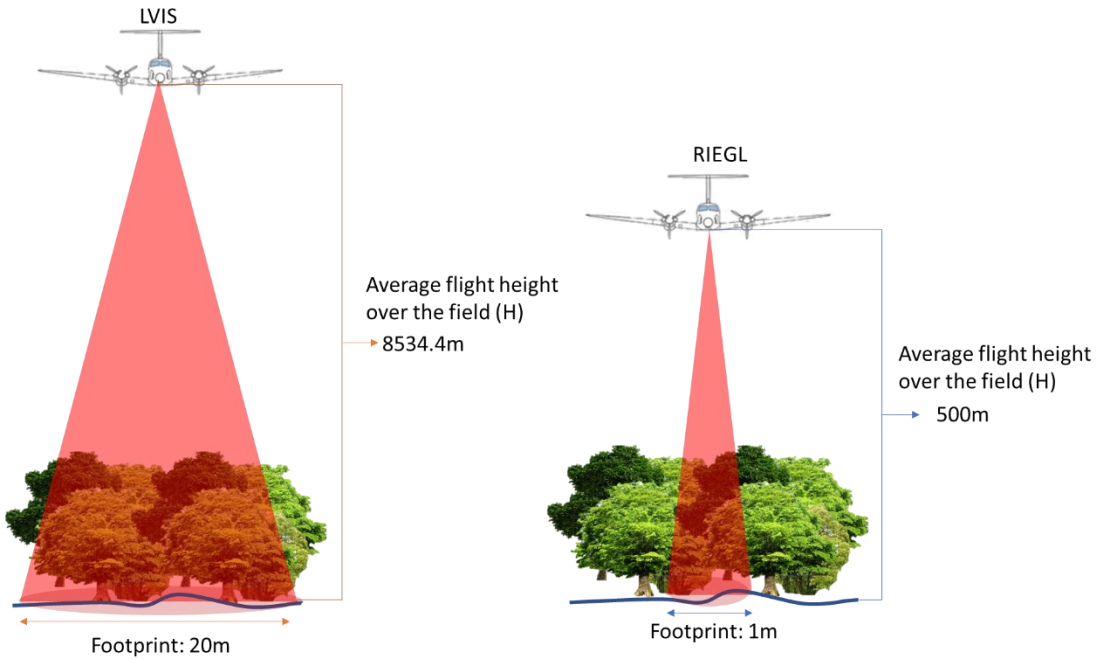


Figure 3. LVIS footprints are recorded with a footprint diameter of 20-meters for the 2005 flight. The RIEGL system used a 1-meter footprint to derive a discrete point cloud from the waveform information in 2021.

The “rGEDl” package was utilized to convert. “las” files (RIEGL) to “.h5” files (LVIS pre-processing files) to obtain comparable data between the two systems (Figure 4). This process included: 1) clipping the RIEGL discrete point cloud within the 20m LVIS footprint, so a point cloud with a radius corresponding to the LVIS can be produced; and 2) using the “rGEDl” package to convert the clipped point cloud to the waveforms with. “.h5” conversion file. The generated files were classified as “synthesized waveform files”.

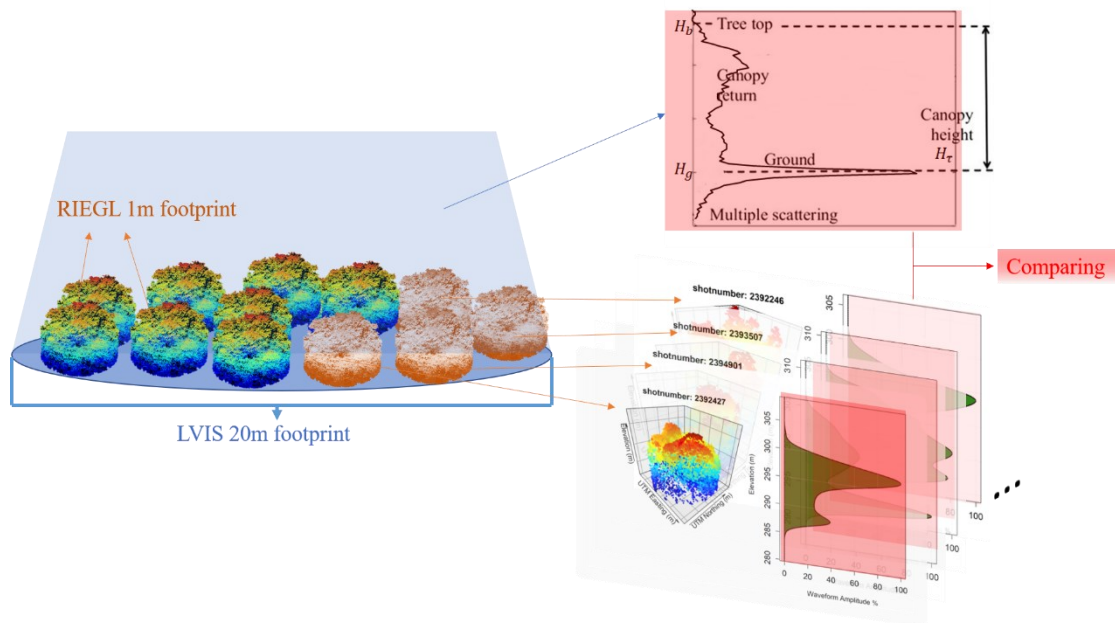


Figure 4. Workflow associated with the processing of the waveforms: 1. The LVIS centroids were located. 2. The discrete point cloud is clipped using the standard LVIS radius. 3. The .h5 files are derived from all of those individual point clouds. Then we compared the LVIS (2005) waveform and the .h5 waveform from RIEGL (2022).

In addition to the digitized waveforms, the original LVIS files contain additional information, including “zt” and “zg,” which correspond to the elevation of the highest detected return and the lowest detected mode, respectively, as well as the mean signal noise level “sigmean.” After noise cancelation, the LVIS waveform is comparable to the converted RIEGL waveform. By matching data in a comparable format, the same approach can be used to analyze the waveforms.

2.5.2.a Tree height from waveform

Forests are distinguished by the fact that the tree height is determined using waveforms. As the full-waveform LiDAR data shows, the height of the tree is the time elapsed between the treetop returns and the ground returns, which can be determined from the distance between the two most prominent peaks in the amplitude waveform. In the different seasons, TDF exhibits distinct variations in ecosystem which are recorded by the LiDAR waveform. Throughout the wet season, an increased number of leaves reflect energy from the TDF canopy, resulting in waveforms (Figure 5) that display a prominent peak within the primary canopy layer. However, in the dry season TDFs experience a significant reduction in leaf coverage, leading to a decrease in canopy returns and energy absorption compared to the rainy season. Consequently, the dominant peak of the waveforms shifts towards ground returns (Figure 6).

More precisely, the commencement of the signal H_b indicates both the initial return and peak of the canopy (Figures 5 and 6) while H_g indicates the second peak of the returning signal, or the signal reflected off the ground. H_τ represents the total height of the tree.

(Eq 2):

$$H_\tau = H_b - H_g \quad (2)$$

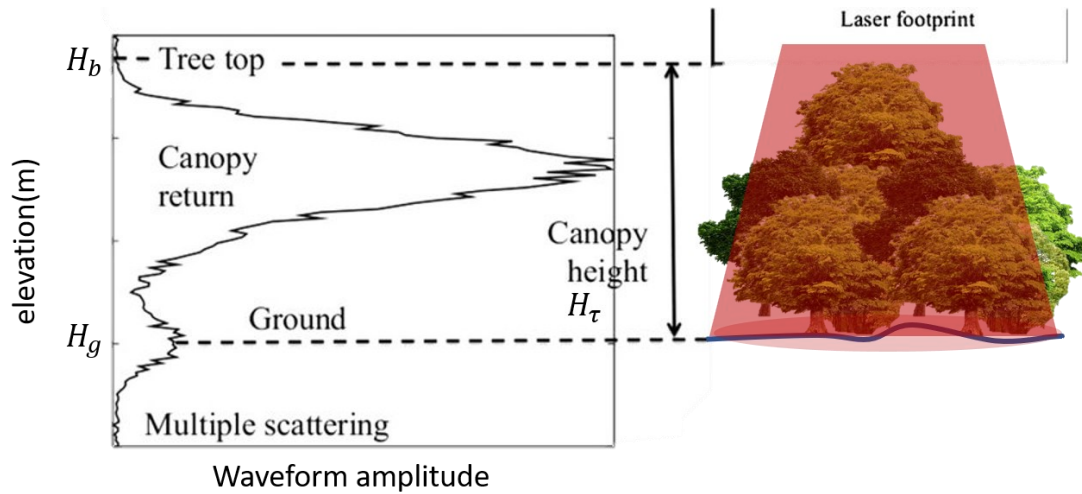


Figure 5. The tree top is the first return represented by H_b , the main ground return is represented by H_g , and H_τ is the tree height during the wet season. During the wet season, more leaves return the energy from the tree top and waveform showing the dominant peak in the main canopy. During the wet season, more leaves return energy from the tree top and waveform, showing a dominant peak in the main canopy.

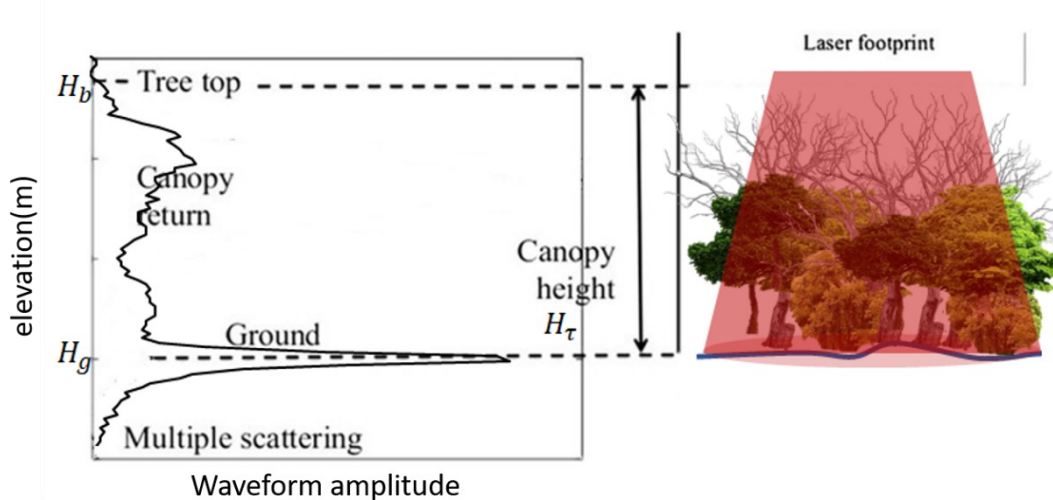


Figure 6. The left figure represents a waveform from the dry season. During this time of year, the TDF's leaves drop substantially, the canopy returns and the energy absorption are lower than during the rainy season. The ground returns from the dominant crest of the waveforms.

According to Roberts (1998), canopy structure (e.g., density and closure) influences the recognition of the highest point of the canopy instead of the highest peak of the largest mode in a waveform. Therefore, to select the ground peak, Harding *et al.*, (2005) specified that the ground surface must be the end-peak of the relative amplitude. They also found that the beginning of the first main peak was at the top of the canopy and the strongest return from the bottom was the ground return. Therefore, it is hypothesized that the RIEGL average tree height ($H_{\tau-RIEGL}$) in 2021 is greater than the LVIS average tree height $H_{\tau-LVIS}$ in 2005.

2.5.2.b Waveform metrics

The most commonly used method for estimating height changes is to calculate the Relative Height (RH) metrics (e.g., RH25, RH50, RH75, and RH100). The vertical heights are denoted as RH25, RH50, RH75, and RH100, based on the vertical distances between the 25%, 50%, 75%, and 100% energy returns. From the LVIS .lge file, the RH metrics are estimated by the function of the z_g value, which is the lowest detected elevation within the waveforms. The z_g values of the REIGL data may be identified using the same approach, notwithstanding the identical scale waveform amplitude, and ensuring that the RH metrics of the two distinct lidar systems are comparable.

The analysis of waveforms requires shape-based metrics, in addition to RH measurements. According to Muss *et al.* (2013), shape-based metrics present a challenge to the standard energy

accumulated approach, specifically in the absence of potential information from the waveform shape and collinearity of the quantile datasets (RH metrics). Using the connection between the shape, location, and wavelength of the LiDAR waveforms, the position of the centroid (C_x and C_y) was computed as a function of the balanced point of the waveforms. The centroid provides more exact and direct information on the position and form of waveforms. In this study, C is relative to the ground, as the detected waveforms indicate that the tree canopy returns to the ground. In addition, the Radius of Gyration (RG) was computed by utilizing the root mean square of the distance between the center of the waveform and its edge to quantify the waveform.

(Eq 3):

$$RG = \sqrt{\frac{\sum(x_i - C_x)^2 + \sum(y_i - C_y)^2}{n}} \quad (3)$$

2.5.2.c Age group and succession stages

Understanding the growth trajectory of secondary forests requires a chronosequence approach, particularly for long-term studies (Quesada et al., 2009). According to Arroyo-Mora *et al.* (2005), successional phases are influenced by vertical and horizontal structures, the dynamics of leaf flushing (leaf on/leaf off), and the density of the green canopy cover. The four stages of succession include pastures, early succession, intermediate succession, and late succession; since 2005, early forests were still a mixture of pasture and trees, and only the changes that occurred during the intermediate and late succession periods have been taken into account.

According to Zhao *et al.* (2021), an age-attributed metric can be used to merge LVIS LiDAR data with hyperspectral information to provide an age map with groups of 0-10 years, 10-20 years, 20-30 years, 30-50 years, and 50+ years. Using Zhao *et al.* (2021) as a reference, we considered three forest age groups: 0-30 years (early) old, 30-50 years (intermediate), and > 50 years (late). Because there were 16 years between images, the age of the forest also changed. Hence, by 2021, each stage (2005) had moved into the next successional stage: the early to intermediate, the intermediate to late, and late stage remained the same. Then we separated the late stage in 2021 to late1 and late2. Late1 is grown from intermediate stage in 2005 and late2 grew from the late stage in 2005.

2.6 Results

2.6.1 Change in relative height traits and canopy height

Table 3 provides the variations in RH metrics relevant to the four succession stages in 2005 and 2021. The RH25 shows slight fluctuations in height between 2005 and 2021, indicative of the fact that, irrespective of the successional stage, the understory vegetation has increased. In contrast, the alterations in the upper canopy are moderate and increase by two to five meters. The transition from early (2005) to intermediate (2021) has the highest rate of change among the four RH metric groups, about four to ten times that of the other groups. As a comparison of the same age group, late (Table 3) and late1 (Table 3) show similar mean RH75 and RH100 values of 11m and 17m, respectively. The trees in the late1 group have already completed the growth transition from intermediate 2005, indicating a high degree of age similarity between the late (2005) and late1 (2021).

Between 2005 and 2021, variations in the mean and standard deviation of the forest's succession stages are observed, particularly for RH25. During the previous 16 years, the move from the late stage to the late2 stage resulted in an increase of six meters across all RH metric categories (6.3%/year). One conspicuous shift is the marked rise in the RH50 of the early stage in 2005, which surged to 6.25 meters by 2021 (6.0%/year), nearly six times its initial height. These findings suggest that tremendous growth and development have transpired within the forest during the specified timeframe. The intermediate to late stages, however, exhibited the least amount of growth over the span of 16 years. This minimal growth, particularly evident in a

mere two-meter increase in RH100. It is, nevertheless, important to realize that the changes between the late stage in 2005 and the late1 stage in 2021 are modest for RH75 and RH100, signaling that the forest has stayed generally homogeneous in these higher RH metric categories. In conclusion, it is obvious that the forest has considerably altered in the early stage during the past sixteen years, while remaining rather stable in the late stage.

Table 3: 2005(LVIS) and 2021(RIEGL) mean Relative Height with the 25%, 50%, 75% and 100% energy back with one standard deviation. Data is grouped as a function of successional stages.

year stage	2005 (LVIS)			2021 (RIEGL)		
	early	intermediate	late	intermediate	late1	late2
RH25 (m)	0.40±0.38	1.25±1.43	2.71±2.39	4.01± 2.10	6.15±2.37	8.43±3.34
RH50 (m)	1.32±1.20	4.21±2.82	6.42±3.88	6.25±2.59	9.30±2.74	12.16±3.60
RH75 (m)	3.39±2.06	8.21±3.31	10.11±4.56	8.18±2.83	11.89±2.87	15.13±3.66
RH100 (m)	9.39±3.21	15.49±3.90	17.11±5.91	13.16±3.10	17.52±3.08	21.28±3.92

Figure 7 presents the density distribution of Canopy Heights (CH) in 2005 and 2021. Maximum of the distributions are observed at 16 and 17 m, respectively. This data is close to the intermediate stage (red) from 15 to 18 m in Figure 8. Nonetheless, there is a substantial variance in CH between 2005 and 2021, with the mean canopy height expanding from 14.2 meters to 17.0 m (2.8 m) over the whole study area about . Figure 7 also shows that for the CH changes in 2005, there is a distinct gap between the 2021 CH from 0 to 11 m, indicating a transition from pasture to an early successional stage not currently observed on the 2005 data.

The intermediate stage (red) in Figure 8 shows CH from the intermediate stage in 2005 to the late1 stage in 2021 for this group. Among the three groups in Table 3 that exhibit a consistent trend in RH100 from the intermediate (2005) to late1 (2021) stages, the trees in this particular group display the least amount of growth variation.

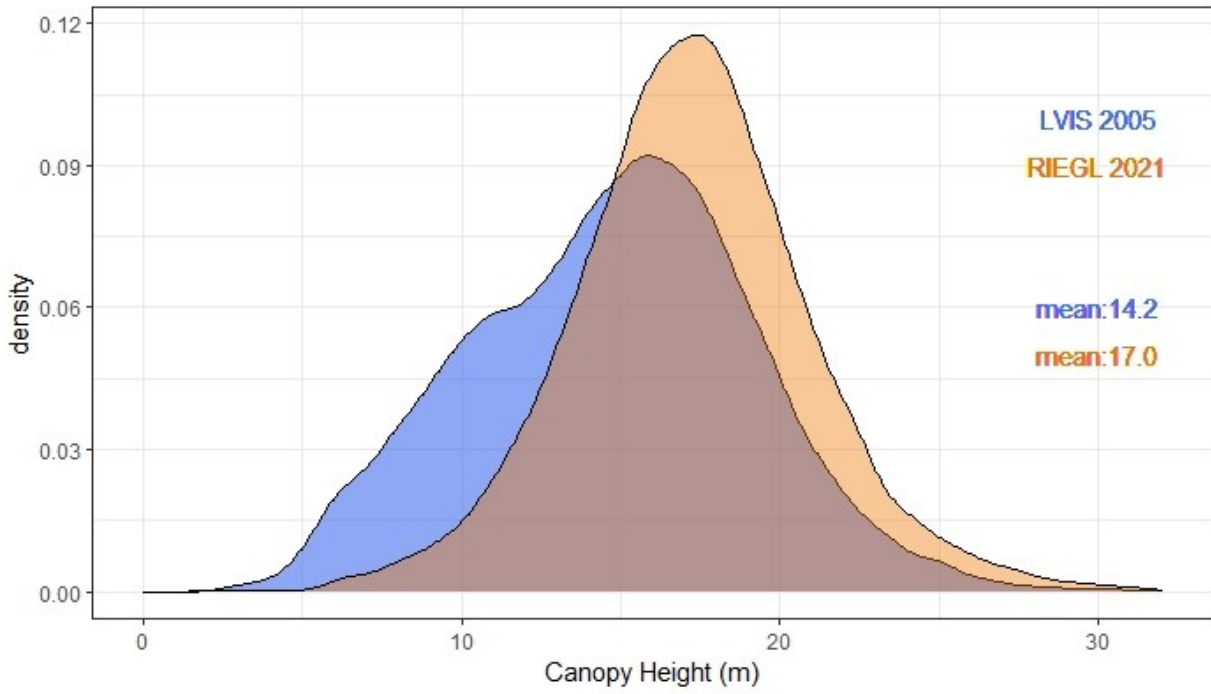


Figure 7. Density chart showing the density of Canopy Heights (CH) in 2005 and 2021. Blue represents the LVIS 2005 and orange represents RIEGL 2021.

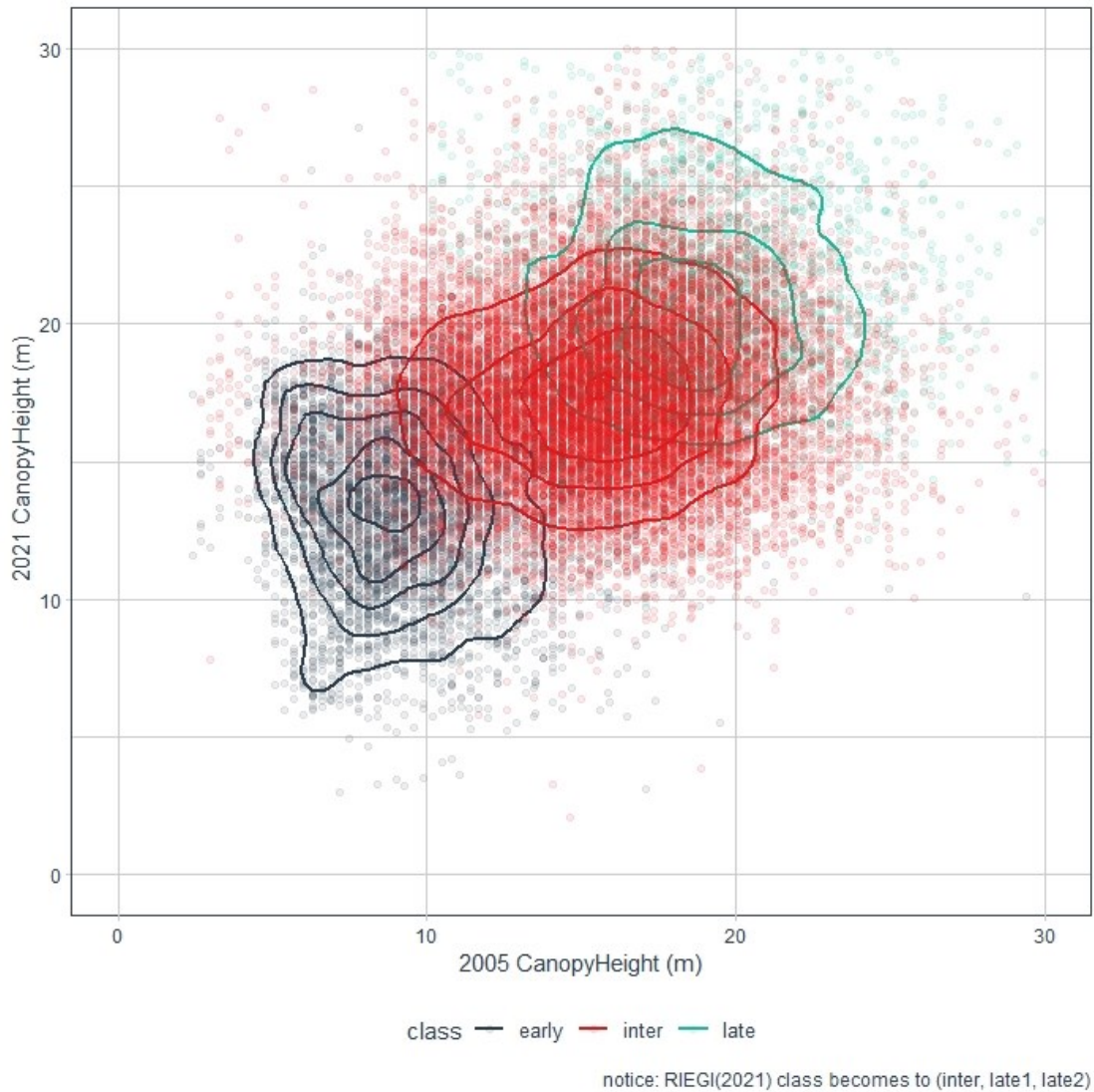


Figure 8. Point graph showing the different Canopy Heights (CH) for the early, intermediate and late successional stages in 2005, and then changes to the intermediate, late1, and late2 stages in 2021. Curved circles represent the density. When circle size increases, a lower density is represented.

2.6.2 Comparison of waveform centroid metrics

Figure 9 presents the different Cx and Cy positions of the three successional stages in 2005. Cx changes between 5-20 and the Cy between 10-20 m. The intermediate stage follows the late stage, and the Cx in this stage is more adaptable, ranging from 10 to 60. The early stage is depicted at the bottom of the graph with an elevation profile that is approximately 4m lower. This is owing to the fact that tree height is lower in the early stage, as demonstrated in the RH metrics of Table 3. Moreover, the intermediate stage dominates the graph, which is consistent with the intermediate stage in Figure 8.

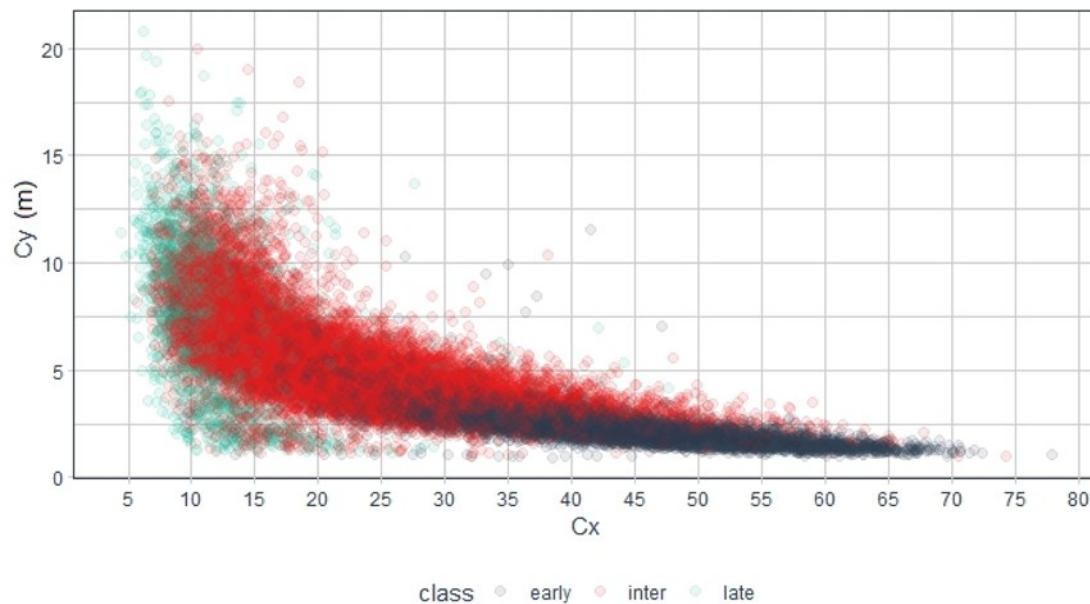


Figure 9. Point graph showing Cx and Cy as representing each footprint's centroid of the 2005 waveforms. Separated colours express the early stage in dark, intermediate stage in red and the late stage in blue.

In Figure 10, which pertains to the year 2021, the primary Cx values exceed 20, indicating a significant decrease compared with the Cx values in 2005 that is related to high ground return in leaf-off season. Additionally, the stages are more distinctly separated, with pronounced margins observed between them. The demarcation between the intermediate stage and late1 stages becomes apparent when Cy attains a value of 7, while the distinction between the late1 and late2 stages becomes apparent at a Cy value of 15. Despite some overlap between the late1 and late2 stages, the majority of the data points are concentrated in the late1 stage.

Furthermore, there is a notable variation in the density of data points among the different growth stages. Specifically, the intermediate stage in 2005 and the late1 stage in 2021 account for the majority of the points. This trend suggests that the trees have undergone considerable growth, resulting in a denser and more layered canopy.

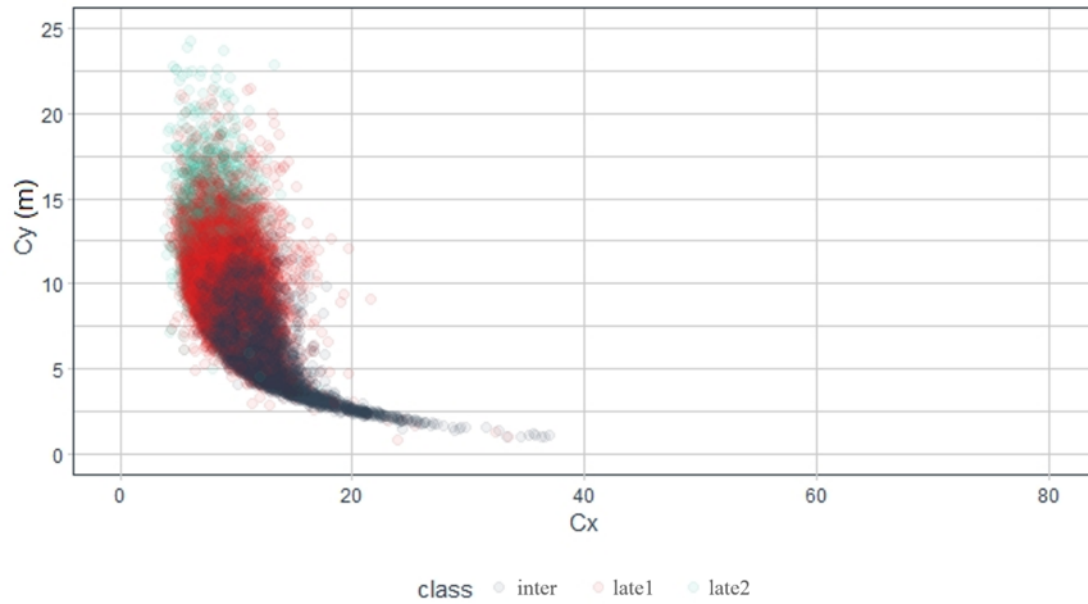


Figure 10. Point graph using Cx and Cy to represent each footprint's centroid of the 2021 waveform. Separated color express the intermidiate stage in dark, the late1 stage in red and the late2 stage in blue.

2.6.3 Comparing waveform line-shape based metrics

In Figure 11, the LVIS (2005) frequency distribution presents a plateau in point density at $Cx = 14$ and continually decreases the density to $Cx = 78$. The highest Cx point density in 2021 is reached at a Cx of 9 waveform amplitude. Simultaneously, the max Cx in 2021 reached 37, which is less than half of the maximum value recorded in 2005, approximately 78. The 2005 waveform surpasses the 2021 data, suggesting that the ground return energy in 2005 was greater than that collected in 2021. The primary factor driving this difference is that the leaf-off season's Cx is typically higher than in the leaf-on season. Consequently, less canopy cover is available to absorb the energy during the leaf-off season.

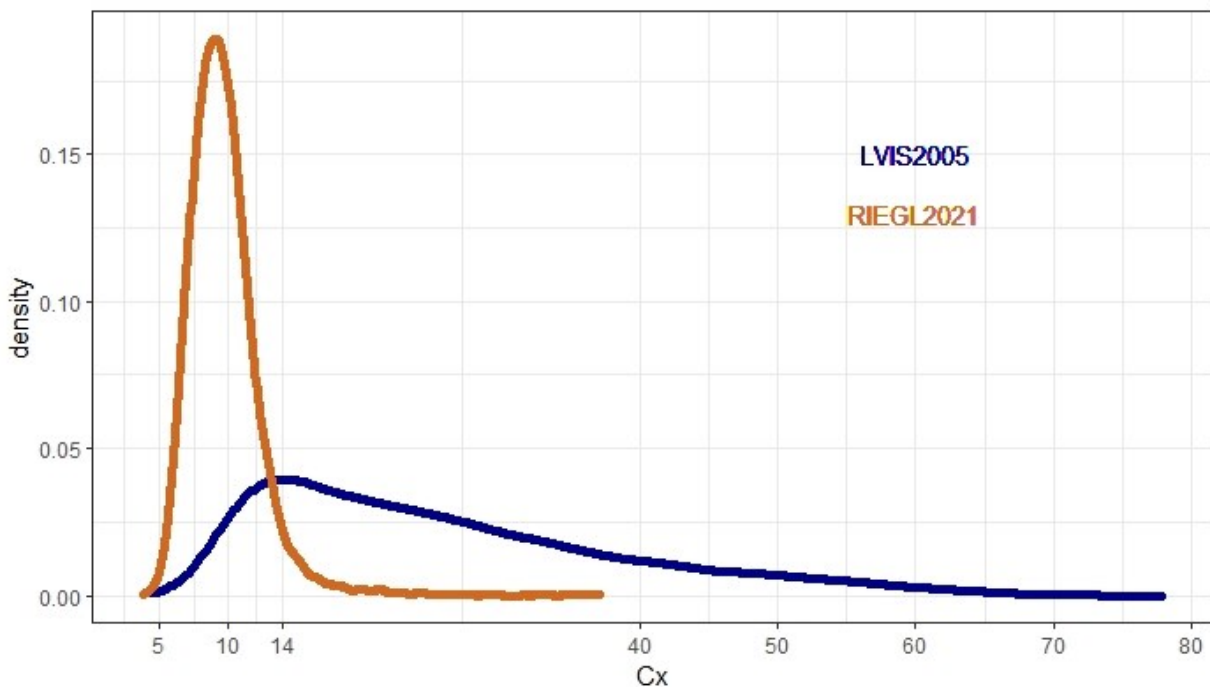


Figure 11. Frequency distribution of Cx illustration changes between 2005 and 2021.

Figure 12 presents a comparison between Cy in 2005 and 2021. The elevation profile is shown by the Y-axis. The data indicates that the 2005 peak is around 3.5 meters in height, whereas the 2021 peak is approximately 9 meters. The graph depicts a changing trend in the line, which, according to waveform analysis, suggests that the vertical profile is rising since the trees have been growing over a period of 16 years.

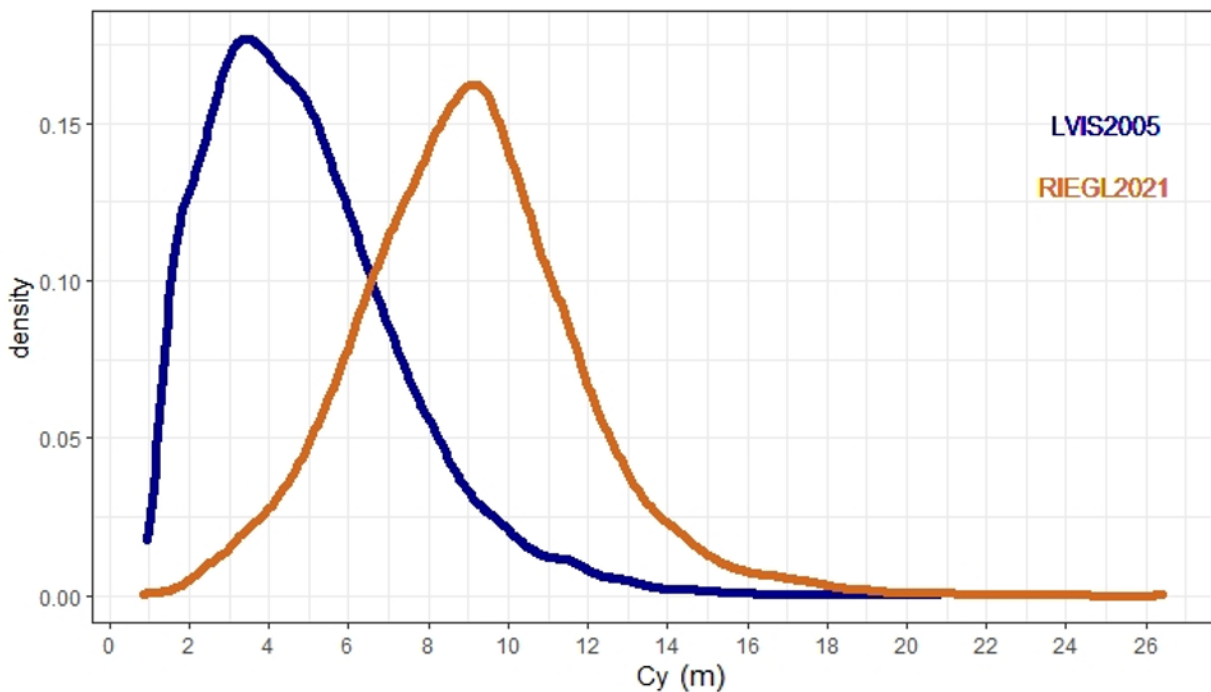


Figure 12. Frequency distribution of Cy illustration changes between 2005 and 2021.

Figure 13 presents a comparison for RG between 2005 and 2021. The 2021 density line demonstrates an upward trend as trees are growing which is expected from an ecological point of view. Figure 13 presents the distribution of RG as a function of successional stage. The tree growth depicted in Figure 14 appears to follow the successional stage group, with the late stage having the highest rate of rise and the highest RG value compared to the early stage in 2005, as indicated by the bottom of the point cloud.

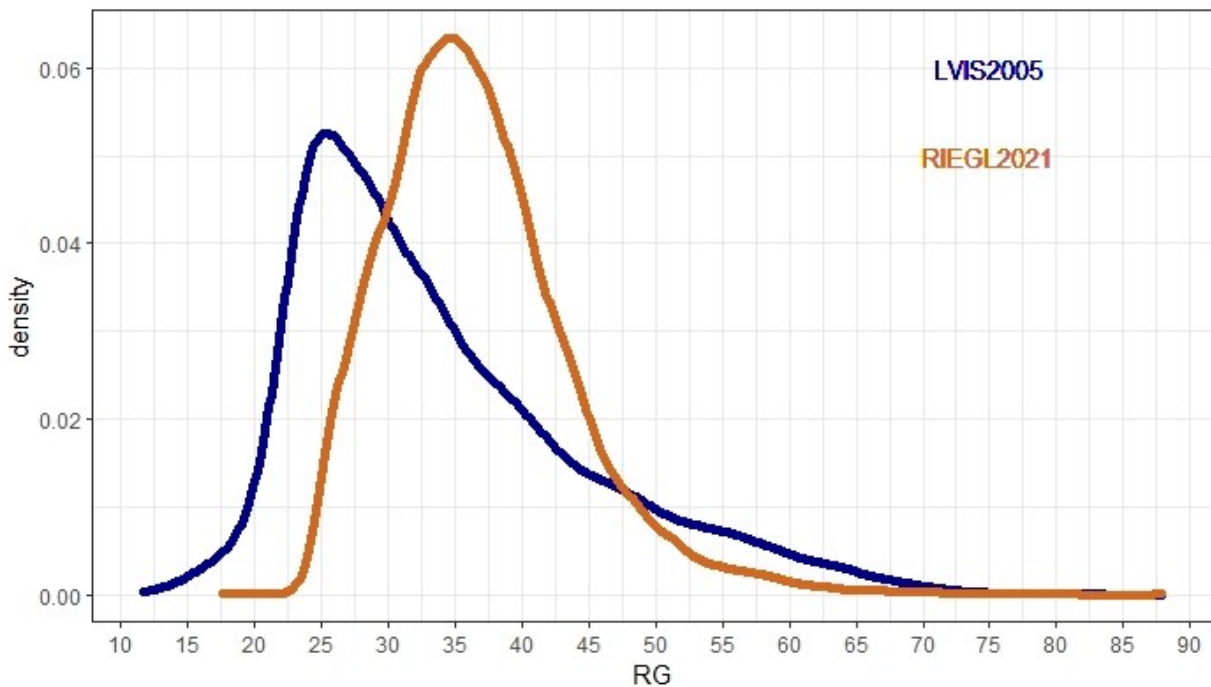


Figure 13. Line graph illustrating the density of the RG distribution in 2005 and 2021.



Figure 14. Point graph showing the RG points grouped by the early, intermediate and late stages. The X axis represent the LVIS 2005 data and the Y axis is RIEGL 2021 data. The color from black, red and blue represent the early stage, intermediate stage, and late stage respectively.

2.6.4 Relation between the metrics

The correlation between several metrics, including Cx, Cy, RG, CH and RH100, in both 2005 and 2021 are depicted in Figure 15 and Figure 16. Of these metrics, the relationship between Cx and RG in Figure 15 stands out, as it indicates a high level of correlation. This is due to the fact that Cx yields a higher value compared to Cy in the calculation of RG, suggesting that ground returns from 2005 are the primary contributor to energy reflectance since the data was collected in dry season. Additionally, Figure 15 shows that the ground returns during the dry season produced the largest peak, which significantly contributed to the Cx calculation.

Figure 15 also reveals favorable correlations between the CH-RH100, Cy-RH100, and Cy-CH connections. This can be attributable to the fact that variations in CH, Cy, and RH100 are connected to differences in the forest's vertical profile. In contrast, RG has a negative correlation with CH, RH100, and Cy, indicating that ground returns are very robust and weaken the link between tree height profiles and ground returns.

Moving on to Figure 16, RG is positively influenced by metrics related to vertical profiles, especially in the range of 0.5-1. This is particularly noticeable in the CH-RH100, RG-RH100, and RG-CH relationships, which display the opposite correlation compared to the 2005 data. The reason for this is that during the leaf-on season, multiple canopy layers contribute significantly to energy reflectance, as shown in Figure 5. Consequently, the waveform peak is dominated by canopy reflectance, and the waveform amplitude related to Cx is negatively related to the remaining four metrics.

Correlation of 2005

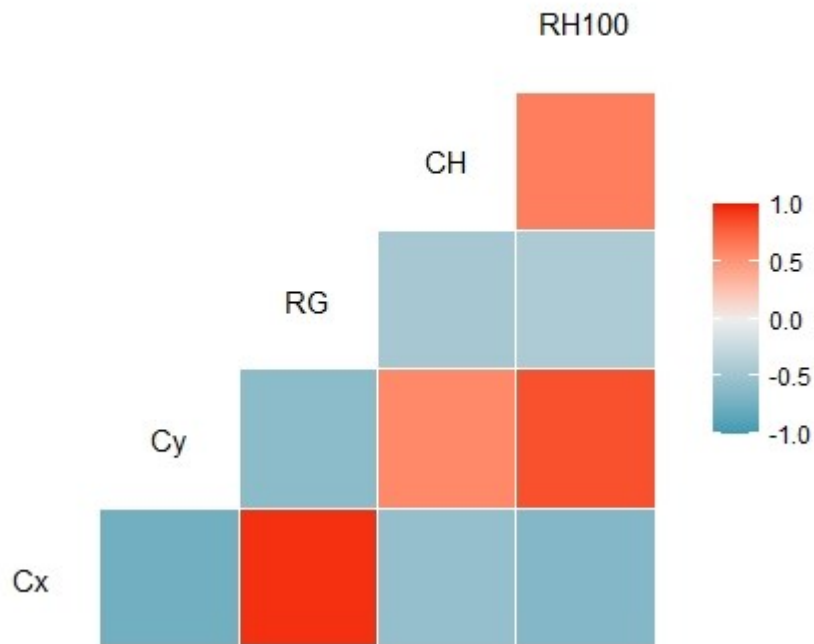


Figure 15. Correlation graph showing the relation between the Cx, Cy, RG, CH and RH100 metrics in 2005. The color gradient represents the degree of positivity or negativity between the measurements. Blue is negative, whereas red is positive.

Correlation of 2021

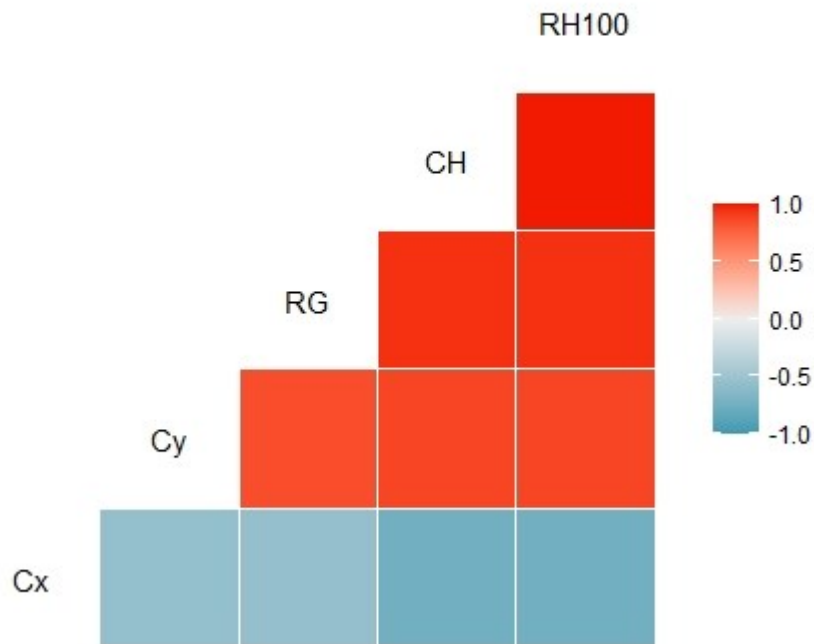


Figure 16. Correlation graph showing the relation between the Cx, Cy, RG, CH and RH100 metrics in 2021. The color gradient represents the degree of positivity or negativity between the measurements. Blue is negative, whereas red is positive.

2.7 Discussion

This study delves into the topic of waveform metrics and their effectiveness in visualizing the evolution of tropical dry forests (TDFs) in Costa Rica over a period of 16 years. This study uses a combination of LVIS and RIEGL data collected in 2005 and 2021, respectively, to provide a comprehensive analysis of the changes that have occurred in TDFs over time.

In recent years, RIEGL data has been gathered, allowing researchers to study the SRNP in greater detail and at a resolution of 1 m. These data offer valuable insights into the potential changes that may have occurred in TDFs over the past 16 years. By analyzing the waveform metrics from both datasets, the study concluded that tree height and canopy height in the SRNP have increased since the initial LVIS data collection in 2005. This study provides vital information to academics, conservationists, and policymakers concerned with the preservation and management of TDFs. Visualizing the variations in TDFs over time using waveform metrics can help identify areas requiring conservation efforts and project the possible effects of climate change and other environmental variables on these ecosystems. This research contributes to our understanding of TDFs and their significance in tropical environments for sustaining biodiversity and ecological balance.

2.7.1 Mapping forest with time series by LiDAR

The results of waveform analysis revealed progressive growth of TDFs at the SRNP. The average canopy height grew by 2.8 meters. The ascending variables are also reflected in the rising RH metrics (Table 3), shifting the Cy density position (Figure 12), increasing RG density (Figure 13), and shifting the Cx and Cy positions (Figure 9 and 10). In Figure 7, an interesting gap appears between the 2021 CH line from 0 m to 11 m, which shows that there may be factors contributing to faster growth or development in early stage compared to the other two successional stages. More related research is required to identify these elements and their possible influence on forest ecosystems.

These findings are consistent with previously published assessments of tropical regions, and our study updates and expands on previous comparisons of canopy height and RH metrics (Gu *et al.*, 2018). Moreover, our work updated the comparison to include not only the RH100 height, but also the RH25, RH50, and RH75 heights, along with showing increases in tree heights across all RH matrices. Mora *et al.*, (2015) found TDFs showed an increase of tree height in the first 3 years and are expected to continue the growing trend for 15 years. The chronosequence model predicts an increasing trend that matches the results of our work in the RH100 comparison (Table 3) and the Cy changes (Figure 12).

Separately, different successional stages showed different rates of increase. The early stage showed the most significant increase in canopy height, with an increase of approximately 4 m

in RH100, whereas the late stage exhibited less growth. Each stage had a unique canopy height range, as demonstrated by Sánchez-Azofeifa *et al.* (2015). It is noticeable that in Figure 8 and Table 3, the intermediate (2005) to late1 (2021) stages show the least variation in growth. This phenomenon can be attributed to the cross-sectional components of the transition zone between the early to intermediate stages and the intermediate to late stages. In other words, the transition from one stage to the next in this group was relatively smooth and consistent, leading to a more uniform growth pattern and less variation among individual trees.

However, we demonstrated here that the early, intermediate, and late stages result in the uniqueness of Cx, Cy, and RG. Although Figures 12 and 13 show some overlapping point data, the separate distribution of each stage point confirms the sensitivity of the shape-based waveform. However, the study of the successional stage is restricted by the difficulty of continuing data collection, which prevents comprehension of the unique dynamics inside the forest, particularly in the transition zone or the border of the age map (Duan *et al.*, 2023). In TDFs, elements such as temperature, humidity, soil moisture, precipitation, and light have a substantial impact on the 16-year growth (Nath *et al.*, 2006). Specifically, Nath *et al.* (2006) identified precipitation, temperature, and soil properties as the primary factors affecting secondary forest development. This study utilized long-term data collected between 1988 and 2000, including parameters such as diameter at breast height (DBH), precipitation, temperature, and soil properties. The data revealed a positive correlation between tree growth and both precipitation and soil moisture but a negative correlation between forest growth and temperature. It is critical to recognize that this research does not account for environmental

changes that may have occurred in Santa Rosa National Park throughout its 16-year expansion period, since these changes were never documented or examined.

At the same time, the uncertainty (overlay part in Figures 9 and 10) of 2021's successional stages is the result of the theoretical chronosequence of forest development. Our study showed only one possible trajectory of TDFs growth. However, Borges *et al.* (2023) suggested a possible method to pursue future estimations based on the similarity of forest growth, regardless of the type of forest. Future studies predicting the future development of TDFs should consider the possible relationship between TDFs and other types of forests.

2.7.2 Seasonal impact of the TDFs comparison

The TDFs exhibit a clear differentiation between the wet and dry seasons. During the wet season, the TDFs experience higher levels of soil moisture and precipitation, which leads to an increased flourishing of the forest in comparison to the dry season. In fact, during the wet season, the TDFs exhibit growth patterns similar to those of wet forests. The growth is slowed, however, and even halted when the dry season arrived (Vieira & Scariot, 2006). This seasonality is evidenced by the findings from the 2005 LVIS (dry season) and the 2021 RIEGL (wet season) studies. Specifically, the growth of TDFs has been observed to be faster during the wet season compared to the dry season (Poorter et al., 2019).

The seasonality of the TDFs also introduces uncertainty into forests studies, which is manifested in the inverse relationship observed in Figure 15 and Figure 16. The reversal of energy returns in the dry season is due to the fact that leaves, which are the primary reflectors of LiDAR signals, are absent during this period. Consequently, the LiDAR system detects mostly ground returns rather than canopy returns, resulting in the observed waveform peak (Figure 6). Conversely, during the wet season, when leaves are present on the trees, the LiDAR system detects mostly canopy returns, leading to the observed major energy occupation by canopies.

Simultaneously, early stage forests are comprised of a dense herbaceous understory and a massive openness canopy of drought deciduous trees (Sánchez-Azofeifa, *et al.*, 2015). The results of the 2005 LVIS contain a large number of early-stage forests, as indicated by the lowest canopy height in Figure 7 and Table 3. On the other hand, the intermediate and late stages have a greater number of fast growing trees, lianas, and evergreen crowns, which offer a thicker canopy to the TDFs in wet season (Zhao, *et al.*, 2021). As a result, the LVIS 2005 early stage waveform displays a greater number of ground returns than the other two stages in the waveform. Compared to data from 2021, the canopy layers absorb more energy since, presumably, there are no early-stage remnants. The waveform of the 2021 wet season resembles the typical forest LiDAR waveform more closely (Figure.4) (Reitberger, *et al.*, 2008).

It is worth noting that the seasonality of TDFs introduces some uncertainty into forest studies.

As mentioned earlier, the absence of leaves during the dry season can lead to high ground

returns and little canopy returns, indicating a lower number of trees or a smaller number of leaves on the trees. This introduces uncertainty into forest studies that rely on LiDAR data, particularly when trying to estimate tree height, tree biomass and carbon storage. Therefore, it is essential to consider seasonality when using LiDAR data for forest studies, and to take measures to account for the absence of leaves during the different seasons.

Furthermore, it is important to note that the resolution of the original data comparison between LVIS and RIEGL is significantly different, with a ratio of 20:1. This represents a considerable upscaling of the data, which may introduce additional noise and uncertainties into the results. Therefore, the potential impact of this upscaling on the data and the resulting interpretations should also be considered and discussed. The study from Silva *et al.*, (2018) pointed out a similar methods to convert the point clouds to waveforms to ensure the small footprint LiDAR system is comparable with large footprints. Silva *et al.*, (2018) discovered that the outcomes of the big and small footprints were comparable, particularly the canopy height and ground elevation. And from the preceding paragraph, the SRNP's TDFs followed a similar pattern of development. As a consequence of our research, it is advisable that future studies compare data from the same season in order to eliminate the influence of the TDFs' seasonality, which has no correlation with the footprint size.

2.8 Conclusion

In this study, the TDFs in Santa Rosa National Park (SRNP) have witnessed growth over 16 years. Based on the Canopy Height, Relative Height, stage group, waveform shape, and line metrics analysis, the following conclusions can be drawn:

With 16 years of growth, TDFs revealed notable variations in height-related profiles, particularly from RH50, RH100, and waveform produced canopy height. Line- and shape-based waveform metrics recorded all changes in the TDFs during the 16 years of growth. Cy and RG increased during forest growth, and Cy showed a positive relationship, particularly in the 2021 wet season results. Cx is shown to have relatively decreased because the ground returns are lower when the canopy density increases and the canopy height increases.

Intermediate (2005) and late1 (2021) stage trees contributed to the main canopy height with the largest number of trees. By 2021, it is rare to notice early-stage forests in TDFs using LiDAR.

The wet and dry seasons in TDFs drive significant changes in the waveform, especially in relation to the Canopy Height and RG. Thus, the same seasonal data introduces fewer influencers in the result, which means that the same season data results are more comparable.

The results of our study demonstrated changes in TDFs levels within 16 years. This is the first study to quantify the chronosequence of TDFs over the long term, which provides a possible trajectory of TDFs' growth at different stages and a reference for future estimation of vegetation structures.

2.9 References

Allen W. (2001). *Green Phoenix: Restoring the Tropical Forests of Guanacaste, Costa Rica*.

New York: Oxford Univ. Press. 310 pp

Arroyo-Mora, J. P., Sánchez-Azofeifa, G. A., Kalacska, M. E., Rivard, B., Calvo-Alvarado, J.

C., & Janzen, D. H. (2005). 'Secondary forest detection in a neotropical dry forest landscape using Landsat 7 ETM+ and IKONOS imagery', *Biotropica*, 37(4), pp. 497–507. doi:

10.1111/j.1744-7429.2005.00068.x.

Borges, S. L. *et al.* (2023) 'Secondary succession in swamp gallery forests along 65 fallow years after shifting cultivation', *Forest Ecology and Management*. Elsevier B.V.,

529(November 2022), p. 120671. doi: 10.1016/j.foreco.2022.120671.

Castillo-Núñez, M. *et al.* (2011) 'Delineation of secondary succession mechanisms for tropical dry forests using LiDAR', *Remote Sensing of Environment*, 115(9), pp. 2217–2231. doi:

10.1016/j.rse.2011.04.020.

Castillo, M. *et al.* (2012) 'LIDAR remote sensing for secondary Tropical Dry Forest

identification', *Remote Sensing of Environment*. Elsevier Inc., 121, pp. 132–143. doi:

10.1016/j.rse.2012.01.012.

Duan, M. *et al.* (2023) 'Characterizing Transitions between Successional Stages in a Tropical Dry Forest Using LiDAR Techniques', *Remote Sensing*, 15(2), pp. 479.

doi:10.3390/rs15020479.

Chitale, V. S. *et al.* (2019) ‘Deciphering plant richness using satellite remote sensing: a study from three biodiversity hotspots’, *Biodiversity and Conservation*. Springer Netherlands, 28(8–9), pp. 2183–2196. doi: 10.1007/s10531-019-01761-4.

Ghulam, A. *et al.*(2014) ‘Detecting subcanopy invasive plant species in tropical rainforest by integrating optical and microwave (InSAR/PolInSAR) remote sensing data, and a decision tree algorithm’, *ISPRS Journal of Photogrammetry and Remote Sensing*. International Society for Photogrammetry and Remote Sensing, Inc. (ISPRS), 88, pp. 174–192. doi: 10.1016/j.isprsjprs.2013.12.007.

Gillespie, T. W. *et al.* (2009) ‘Towards quantifying tropical tree species richness in tropical forests’, *International Journal of Remote Sensing*, 30(6), pp. 1629–1634. doi: 10.1080/01431160802524552.

Gu, Z. *et al.* (2018) ‘Using LiDAR waveform metrics to describe and identify successional stages of tropical dry forests’, *International Journal of Applied Earth Observation and Geoinformation*. Elsevier, 73(January), pp. 482–492. doi: 10.1016/j.jag.2018.07.010.

Harding, D.J. and Carabajal, C.C. (2005) ‘ICESat waveform measurements of within-footprint topographic relief and vegetation vertical structure’, *Geophysical Research Letters*, 32(21), pp. 1–4. doi:10.1029/2005GL023471.

Janzen, D. H. (2000) ‘Costa Rica’s Area de Conservación Guanacaste: A long march to survival through non-damaging biodevelopment’, *Biodiversity*, 1(2), pp. 7–20. doi: 10.1080/14888386.2000.9712501.

- Kennard, D. K. (2002) 'Secondary forest succession in a tropical dry forest: Patterns of development across a 50-year chronosequence in lowland Bolivia', *Journal of Tropical Ecology*, 18(1), pp. 53–66. doi: 10.1017/S0266467402002031.
- Li, W. *et al.* (2017) 'Identifying tropical dry forests extent and succession via the use of machine learning techniques', *International Journal of Applied Earth Observation and Geoinformation*. Elsevier, 63(August), pp. 196–205. doi: 10.1016/j.jag.2017.08.003.
- Marín, G. C. *et al.* (2005) 'Stand dynamics and basal area change in a tropical dry forest reserve in Nicaragua', *Forest Ecology and Management*, 208(1–3), pp. 63–75. doi: 10.1016/j.foreco.2004.10.072.
- Martinuzzi, S. *et al.* (2013) 'Quantifying Tropical Dry Forest Type and Succession: Substantial Improvement with LiDAR', *Biotropica*, 45(2), pp. 135–146. doi: 10.1111/j.1744-7429.2012.00904.x.
- Meléndez Chaverri, C. (1974). *Viajeros por Guanacaste microform: [relatos]*. Ministerio de Cultura: Juventud y Deportes, Departamento de Publicaciones, San José, Costa Rica.
- Mora, F. *et al.* (2015) 'Testing Chronosequences through Dynamic Approaches: Time and Site Effects on Tropical Dry Forest Succession', *Biotropica*, 47(1), pp. 38–48. doi: 10.1111/btp.12187.
- Muss, J. D. *et al.* (2013) 'Analysis of waveform lidar data using shape-based metrics', *IEEE Geoscience and Remote Sensing Letters*, 10(1), pp. 106–110. doi: 10.1109/LGRS.2012.2194472.

Nath, C.D. et al. (2006) 'Patterns of tree growth in relation to environmental variability in the tropical dry deciduous forest at Mudumalai, southern India', *Journal of Biosciences*, 31(5), pp. 651–669. doi:10.1007/BF02708418.

Park, H. J. *et al.* (2011) 'Analysis of pine tree height estimation using full waveform lidar', 34th International Symposium on Remote Sensing of Environment - The GEOSS Era: Towards Operational Environmental Monitoring, Sydney Australia, pp. 3–6.

Phillips, J. D. *et al.* (2017) 'Domination of hillslope denudation by tree uprooting in an old-growth forest', *Geomorphology*, 276, pp. 27–36. doi: 10.1016/j.geomorph.2016.10.006.

Pirotti, F. (2011). Analysis of full-waveform LiDAR data for forestry applications: a review of investigations and methods. *iForest-Biogeosciences and Forestry*, 4(3), pp. 100–106. doi: 10.3832/ifor0562-004.

Poorter, L. *et al.* (2019) 'Wet and dry tropical forests show opposite successional pathways in wood density but converge over time', *Nature Ecology and Evolution*. Nature Publishing Group, 3(6), pp. 928–934. doi: 10.1038/s41559-019-0882-6.

Quesada, M. *et al.* (2009) 'Forest Ecology and Management Succession and management of tropical dry forests in the Americas : Review and new perspectives', 258, pp. 1014–1024. doi: 10.1016/j.foreco.2009.06.023.

Reitberger, J., Krzystek, P. and Stilla, U. (2008) 'Analysis of full waveform LIDAR data for the classification of deciduous and coniferous trees', *International Journal of Remote Sensing*, 29(5), pp. 1407–1431. doi: 10.1080/01431160701736448.

- Roberts, D.A. et al. (1998) ‘Spectral changes with leaf aging in Amazon caatinga’, *Trees - Structure and Function*, 12(6), pp. 315–325. doi:10.1007/s004680050157.
- Sánchez-Azofeifa, A., Portillo-Quintero, C. and Durán, S. M. (2015) ‘Structural effects of liana presence Structural effects of liana presence in secondary tropical dry forests using ground LiDAR Structural effects of liana presence’, *Biogeosciences Discuss*, 12, pp. 17153–17175. doi: 10.5194/bgd-12-17153-2015.
- Sánchez-Azofeifa, G. A. *et al.* (2005) ‘Research priorities for neotropical dry forests’, *Biotropica*, 37(4), pp. 477–485. doi: 10.1111/j.1744-7429.2005.00066.x.
- Schneider, F. D. *et al.* (2014) ‘Simulating imaging spectrometer data: 3D forest modeling based on LiDAR and in situ data’, *Remote Sensing of Environment*. Elsevier Inc., 152, pp. 235–250. doi: 10.1016/j.rse.2014.06.015.
- Silva, C. A. *et al.* (2018) ‘Comparison of Small- and Large-Footprint Lidar Characterization of Tropical Forest Aboveground Structure and Biomass : A Case Study From Central Gabon’, *IEEE Journal of Selected Topics in Applied Earth Observations and Remote Sensing*, IEEE, 11(10), pp. 3512–3526. doi: 10.1109/JSTARS.2018.2816962.
- Siyum, Z.G. (2020) ‘Tropical dry forest dynamics in the context of climate change: syntheses of drivers, gaps, and management perspectives’, *Ecological Processes*, 9(1). doi:10.1186/s13717-020-00229-6.
- Solberg, S. *et al.* (2017) ‘Biomass and InSAR height relationship in a dense tropical forest’, *Remote Sensing of Environment*. Elsevier Inc., 192, pp. 166–175. doi: 10.1016/j.rse.2017.02.010.

Stan, K. and Sanchez-Azofeifa, A. (2019) 'Tropical dry forest diversity, climatic response, and resilience in a changing climate', *Forests*, 10(5), pp. 443. doi: 10.3390/f10050443.

Vieira, D. L. M. and Scariot, A. (2006) 'Principles of natural regeneration of tropical dry forests for restoration', *Restoration Ecology*, 14(1), pp. 11–20. doi: 10.1111/j.1526-100X.2006.00100.x.

Zhao, G. et al. (2021) 'Hyperspectral and Full-Waveform LiDAR Improve Mapping of Tropical Dry Forest' s Successional Stages', *Remote Sensing*, 13(19), pp. 1–27. doi:10.3390/rs13193830.

3.0 Conclusion

3.1 Summary and contribution

The aim of this study was to advance the understanding of chronosequence changes in Tropical Dry Forests by analyzing different waveform metrics. In conclusion, this study offers valuable insights into the growth of secondary tropical dry forests (TDFs) in Santa Rosa National Park (SRNP) over a 16-year period. Using a range of metrics, including Canopy Height, Relative Height, waveform shape, and line metrics, the study revealed notable variations in the height-related profile of TDFs, particularly in RH50, RH100, and waveform produced Canopy Height. Compared with the research by Mora *et al.* (2015), this study is the first to visualize long-term differences and changes in the forest instead of using chronosequence model estimation. The results show that line- and shape-based waveform metrics recorded all changes in the TDFs during 16 years of growth, with the Cy and RG increasing during the growth of the dry forest canopies and Cy showing a positive relationship, especially in the 2021 wet season results. However, Cx relatively decreased because of the lower ground returns when the canopy density increased and canopy height increased. This research continued the study by Gu *et al.*,(2018), who first identified the successional stages using waveform metrics. The study also found that intermediate (2005) and late1 (2021) stage trees contribute to the main canopy height with the largest number of trees, and by 2021, the early stage forest in TDFs is rare to notice from the LiDAR. Furthermore, wet and dry seasons in TDFs drive significant changes in the waveform, particularly in relation to canopy height and RG, emphasizing the need to consider seasonal data when making comparisons.

In addition to being threatened by human activities and natural disturbances, TDFs are highly valued for their ecological significance. They are home to a diverse range of plant and animal species, many of which are both endemic and endangered (Portillo-Quintero *et al.* 2010). TDFs also play an important role in regulating global climate, as they sequester carbon from the atmosphere and help mitigate the effects of climate change (Le Qu'ér'e *et al.*, 2015; Reyes-Palomeque *et al.*, 2021). Despite their ecological importance and value, TDFs remain among the least protected ecosystems in the tropics, and urgent action is needed to protect and conserve them for future generations (Sánchez-Azofeifa *et al.*, 2015). Although TDFs are more fragile and occupy a larger area, research on their dynamics and secondary successional changes lags behind that of Tropical Wet Forests (Dupuy *et al.*, 2012). The findings of this study have important implications for the management and conservation of TDFs.

The significant variations observed in the height-related profile of TDFs suggest that these forests are not static but undergo dynamic changes over time (Lebrija-Trejos *et al.*, 2010). Therefore, it is crucial to monitor TDFs regularly using LiDAR and other remote sensing technologies to track their growth and assess the impact of environmental factors, such as wet and dry seasons. This study also highlights the importance of considering the stage of the forest when analyzing canopy height, as intermediate- and late-stage trees contribute the most to canopy height. Finally, the results emphasize the need to compare the TDFs data collected during the same season to accurately assess changes over time.

These results have important implications for the management and conservation of TDFs, highlighting the need for regular monitoring using remote sensing technologies and the importance of considering the successional stage of the forest and seasonal changes when analyzing canopy height. Through temporal data comparisons, this study underscores the importance of continued research and monitoring of TDFs to ensure their long-term sustainability and conservation.

3.2 Future work

Despite the promising results of the current study, there is still much to be done to better understand the dynamics of secondary TDFs in Santa Rosa National Park (SRNP) and their response to environmental changes. One important avenue for future research is to collect more detailed annual data on TDFs, including canopy height, to better capture changes over time. This will provide a more comprehensive understanding of the growth patterns and responses of TDFs to environmental change.

Another important consideration for future research is ensuring that data from the same season are more comparable. As noted in the current study, the wet and dry seasons caused significant changes in waveform and canopy height. Therefore, to accurately capture and compare the growth patterns and changes in TDFs over time, it is important to collect data at the same time of the year to minimize seasonal variation. This will help ensure that the data collected are comparable across years and seasons.

Overall, future studies should attempt to provide a deeper understanding of the developmental patterns and environmental responses of TDFs. This may be accomplished by collecting more precise and similar data and studying the responses of TDFs to various environmental stresses. Such studies are essential for the development of effective management techniques that can conserve and safeguard TDFs in SRNP and other locations with comparable characteristics.

3.3 References

- Dupuy, J. M. *et al.* (2012) 'Patterns and Correlates of Tropical Dry Forest Structure and Composition in a Highly Replicated Chronosequence in Yucatan, Mexico', *Biotropica*, 44(2), pp. 151–162. doi: 10.1111/j.1744-7429.2011.00783.x.
- Gu, Z. *et al.* (2018) 'Using LiDAR waveform metrics to describe and identify successional stages of tropical dry forests', *International Journal of Applied Earth Observation and Geoinformation*. Elsevier, 73(January), pp. 482–492. doi: 10.1016/j.jag.2018.07.010.
- Lebrija-Trejos, E. *et al.* (2010) 'Pathways, mechanisms and predictability of vegetation change during tropical dry forest succession', *Perspectives in Plant Ecology, Evolution and Systematics*. Elsevier GmbH., 12(4), pp. 267–275. doi: 10.1016/j.ppees.2010.09.002.
- Le Quéré, C. *et al.* (2015) 'Global Carbon Budget 2015', *Earth System Science Data*, 7(2), pp. 349–396. doi: 10.5194/essd-7-349-2015.
- Mora, F. *et al.* (2015) 'Testing Chronosequences through Dynamic Approaches: Time and Site Effects on Tropical Dry Forest Succession', *Biotropica*, 47(1), pp. 38–48. doi: 10.1111/btp.12187.
- Portillo-Quintero, C. A. *et al.* (2010) 'Extent and conservation of tropical dry forests in the Americas', *Biological Conservation*, 143(1), pp. 144–155. doi: 10.1016/j.biocon.2009.09.020.
- Reyes-Palomeque, G. *et al.* (2021) 'Mapping forest age and characterizing vegetation structure and species composition in tropical dry forests', *Ecological Indicators*, 120, pp. 106955. doi: 10.1016/j.ecolind.2020.106955.

Sánchez-Azofeifa, A., Portillo-Quintero, C. and Durán, S. M. (2015) ‘Structural effects of liana presence Structural effects of liana presence in secondary tropical dry forests using ground LiDAR Structural effects of liana presence’, *Biogeosciences Discuss*, 12, pp. 17153–17175. doi: 10.5194/bgd-12-17153-2015.

References

- Allen W. (2001). *Green Phoenix: Restoring the Tropical Forests of Guanacaste, Costa Rica*. New York: Oxford Univ. Press. 310 pp
- Almeida, D.R.A. et al. (2019) ‘Monitoring the structure of forest restoration plantations with a drone-lidar system’, *International Journal of Applied Earth Observation and Geoinformation*, 79(March), pp. 192–198. doi:10.1016/j.jag.2019.03.014.
- Arroyo-Mora, J. P., Sánchez-Azofeifa, G. A., Kalacska, M. E., Rivard, B., Calvo-Alvarado, J. C., & Janzen, D. H. (2005). ‘Secondary forest detection in a neotropical dry forest landscape using Landsat 7 ETM+ and IKONOS imagery’, *Biotropica*, 37(4), pp. 497–507. doi: 10.1111/j.1744-7429.2005.00068.x.
- Asner, G.P. and Mascaro, J. (2014) ‘Mapping tropical forest carbon: Calibrating plot estimates to a simple LiDAR metric’, *Remote Sensing of Environment*, 140, pp. 614–624. doi:10.1016/j.rse.2013.09.023.
- Borges, S. L. *et al.* (2023) ‘Secondary succession in swamp gallery forests along 65 fallow years after shifting cultivation’, *Forest Ecology and Management*. Elsevier B.V., 529(November 2022), p. 120671. doi: 10.1016/j.foreco.2022.120671.
- Castillo-Núñez, M. *et al.* (2011) ‘Delineation of secondary succession mechanisms for tropical dry forests using LiDAR’, *Remote Sensing of Environment*, 115(9), pp. 2217–2231. doi: 10.1016/j.rse.2011.04.020.

- Calvo-Rodriguez, S. *et al.* (2017) 'Changes in forest structure and composition in a successional tropical dry forest', *Revista Forestal Mesoamericana Kurú*, 14(35), p. 12. doi: 10.18845/rfmk.v14i35.3149.
- Castillo, M. *et al.* (2012) 'LIDAR remote sensing for secondary Tropical Dry Forest identification', *Remote Sensing of Environment*. Elsevier Inc., 121, pp. 132–143. doi: 10.1016/j.rse.2012.01.012.
- Cavender-Bares, *et al.* (2020) Remote sensing of plant biodiversity, *Remote Sensing of Plant Biodiversity*, pp. 581. doi: 10.1007/978-3-030-33157-3.
- Clark, M. L. *et al.* (2011) 'Estimation of tropical rain forest aboveground biomass with small-footprint lidar and hyperspectral sensors', *Remote Sensing of Environment*, 115(11), pp. 2931–2942. doi: 10.1016/j.rse.2010.08.029.
- Chitale, V. S. *et al.* (2019) 'Deciphering plant richness using satellite remote sensing: a study from three biodiversity hotspots', *Biodiversity and Conservation*. Springer Netherlands, 28(8–9), pp. 2183–2196. doi: 10.1007/s10531-019-01761-4.
- Duan, M. *et al.* (2023) 'Characterizing Transitions between Successional Stages in a Tropical Dry Forest Using LiDAR Techniques', *Remote Sensing*, 15(2), pp. 479. doi:10.3390/rs15020479.
- Dupuy, J. M. *et al.* (2012) 'Patterns and Correlates of Tropical Dry Forest Structure and Composition in a Highly Replicated Chronosequence in Yucatan, Mexico', *Biotropica*, 44(2), pp. 151–162. doi: 10.1111/j.1744-7429.2011.00783.x.

Falcão, H. M. *et al.* (2015) ‘Phenotypic plasticity and ecophysiological strategies in a tropical dry forest chronosequence: A study case with *Poincianella pyramidalis*’, *Forest Ecology and Management*, 340, pp. 62–69. doi: 10.1016/j.foreco.2014.12.029.

Fedrigo, M. *et al.* (2018) ‘Predicting temperate forest stand types using only structural profiles from discrete return airborne lidar’, *ISPRS Journal of Photogrammetry and Remote Sensing*. Elsevier B.V., 136, pp. 106–119. doi: 10.1016/j.isprsjprs.2017.11.018.

Fieber, K. D. *et al.* (2015) ‘Validation of Canopy Height Profile methodology for small-footprint full-waveform airborne LiDAR data in a discontinuous canopy environment’, *ISPRS Journal of Photogrammetry and Remote Sensing*. Elsevier B.V., 104, pp. 144–157. doi: 10.1016/j.isprsjprs.2015.03.001.

Ghulam, A. *et al.* (2014) ‘Detecting subcanopy invasive plant species in tropical rainforest by integrating optical and microwave (InSAR/PolInSAR) remote sensing data, and a decision tree algorithm’, *ISPRS Journal of Photogrammetry and Remote Sensing*. International Society for Photogrammetry and Remote Sensing, Inc. (ISPRS), 88, pp. 174–192. doi: 10.1016/j.isprsjprs.2013.12.007.

Gillespie, T. W. *et al.* (2009) ‘Towards quantifying tropical tree species richness in tropical forests’, *International Journal of Remote Sensing*, 30(6), pp. 1629–1634. doi: 10.1080/01431160802524552.

Gu, Z. *et al.* (2018) ‘Using LiDAR waveform metrics to describe and identify successional stages of tropical dry forests’, *International Journal of Applied Earth Observation and Geoinformation*. Elsevier, 73(January), pp. 482–492. doi: 10.1016/j.jag.2018.07.010.

Harding, D.J. and Carabajal, C.C. (2005) 'ICESat waveform measurements of within-footprint topographic relief and vegetation vertical structure', *Geophysical Research Letters*, 32(21), pp. 1–4. doi:10.1029/2005GL023471.

Huang, W. *et al.* (2012) 'Mapping forest above-ground biomass and its changes from LVIS waveform data', *International Geoscience and Remote Sensing Symposium (IGARSS)*. IEEE, pp. 6561–6564. doi: 10.1109/IGARSS.2012.6352096.

Jalobeanu, A. *et al.* (2012) The full-waveform LiDAR Riegl LMS-Q680I: From reverse engineering to sensor modeling Coastal Monitoring using UASs View project Accuracy and effectiveness of orthophotos obtained from low cost UASs video imagery for traffic accident scenes documentation View project. Available at:
<https://www.researchgate.net/publication/267556394>.

Jaramillo, V. J. *et al.* (2003) 'Biomass, Carbon, and Nitrogen Pools in Mexican Tropical Dry Forest Landscapes', *Ecosystems*, 6(7), pp. 609–629. doi: 10.1007/s10021-002-0195-4.

Janzen, D. H. (2000) 'Costa Rica's Area de Conservación Guanacaste: A long march to survival through non-damaging biodevelopment', *Biodiversity*, 1(2), pp. 7–20. doi: 10.1080/14888386.2000.9712501.

Kalacska, M. *et al.* (2004) 'Species composition, similarity and diversity in three successional stages of a seasonally dry tropical forest', *Forest Ecology and Management*, 200(1–3), pp. 227–247. doi: 10.1016/j.foreco.2004.07.001.

Kennard, D. K. (2002) 'Secondary forest succession in a tropical dry forest: Patterns of development across a 50-year chronosequence in lowland Bolivia', *Journal of Tropical Ecology*, 18(1), pp. 53–66. doi: 10.1017/S0266467402002031.

Lebrija-Trejos, E. *et al.* (2011) 'Environmental changes during secondary succession in a tropical dry forest in Mexico', *Journal of Tropical Ecology*, 27(5), pp. 477–489. doi:10.1017/S0266467411000253.

Lebrija-Trejos, E. *et al.* (2010) 'Pathways, mechanisms and predictability of vegetation change during tropical dry forest succession', *Perspectives in Plant Ecology, Evolution and Systematics*. Elsevier GmbH., 12(4), pp. 267–275. doi: 10.1016/j.ppees.2010.09.002.

Le Quéré, C. *et al.* (2015) 'Global Carbon Budget 2015', *Earth System Science Data*, 7(2), pp. 349–396. doi: 10.5194/essd-7-349-2015.

Li, W. *et al.* (2017) 'Identifying tropical dry forests extent and succession via the use of machine learning techniques', *International Journal of Applied Earth Observation and Geoinformation*. Elsevier, 63(August), pp. 196–205. doi: 10.1016/j.jag.2017.08.003.

Marín, G. C. *et al.* (2005) 'Stand dynamics and basal area change in a tropical dry forest reserve in Nicaragua', *Forest Ecology and Management*, 208(1–3), pp. 63–75. doi: 10.1016/j.foreco.2004.10.072.

Martinuzzi, S. *et al.* (2013) 'Quantifying Tropical Dry Forest Type and Succession: Substantial Improvement with LiDAR', *Biotropica*, 45(2), pp. 135–146. doi: 10.1111/j.1744-7429.2012.00904.x.

McCombs, J. W. *et al.* (2003) 'Influence of fusing lidar and multispectral imagery on remotely sensed estimates of stand density and mean tree height in a managed loblolly pine plantation', *Forest Science*, 49(3), pp. 457–466. doi: 10.1093/forestscience/49.3.457.

McLaren, K.P. *et al.* (2003) 'The effects of moisture and shade on seed germination and seedling survival in a tropical dry forest in Jamaica', *Forest Ecology and Management*, 183(1–3), pp. 61–75. doi:10.1016/S0378-1127(03)00100-2.

Meléndez Chaverri, C. (1974). *Viajeros por Guanacaste microform: [relatos]*. Ministerio de Cultura: Juventud y Deportes, Departamento de Publicaciones, San José, Costa Rica.

Mora, F. *et al.* (2015) 'Testing Chronosequences through Dynamic Approaches: Time and Site Effects on Tropical Dry Forest Succession', *Biotropica*, 47(1), pp. 38–48. doi: 10.1111/btp.12187.

Muss, J. D. *et al.* (2013) 'Analysis of waveform lidar data using shape-based metrics', *IEEE Geoscience and Remote Sensing Letters*, 10(1), pp. 106–110. doi: 10.1109/LGRS.2012.2194472.

Murphy, P.G. (2008) 'Ecology of Tropical Dry Forest Author (s): Peter G . Murphy and Ariel E . Lugo Source : Annual Review of Ecology and Systematics , Vol . 17 , (1986), pp . 67-88 Published by : Annual Reviews Stable URL : <http://www.jstor.org/stable/2096989>', *Ecology*, 17(1986), pp. 67–88.

Nath, C.D. *et al.* (2006) 'Patterns of tree growth in relation to environmental variability in the tropical dry deciduous forest at Mudumalai, southern India', *Journal of Biosciences*, 31(5), pp. 651–669. doi:10.1007/BF02708418.

Park, H. J. *et al.* (2011) ‘Analysis of pine tree height estimation using full waveform lidar’, 34th International Symposium on Remote Sensing of Environment - The GEOSS Era: Towards Operational Environmental Monitoring, Sydney Australia, pp. 3–6.

Phillips, J. D. *et al.* (2017) ‘Domination of hillslope denudation by tree uprooting in an old-growth forest’, *Geomorphology*, 276, pp. 27–36. doi: 10.1016/j.geomorph.2016.10.006.

Pirotti, F. (2011). Analysis of full-waveform LiDAR data for forestry applications: a review of investigations and methods. *iForest-Biogeosciences and Forestry*, 4(3), pp. 100–106. doi: 10.3832/ifor0562-004.

Poorter, L. *et al.* (2019) ‘Wet and dry tropical forests show opposite successional pathways in wood density but converge over time’, *Nature Ecology and Evolution*. Nature Publishing Group, 3(6), pp. 928–934. doi: 10.1038/s41559-019-0882-6.

Portillo-Quintero, C. A. *et al.* (2010) ‘Extent and conservation of tropical dry forests in the Americas’, *Biological Conservation*, 143(1), pp. 144–155. doi: 10.1016/j.biocon.2009.09.020.

Quesada, M. *et al.* (2009) ‘Forest Ecology and Management Succession and management of tropical dry forests in the Americas : Review and new perspectives’, 258, pp. 1014–1024. doi: 10.1016/j.foreco.2009.06.023.

Reitberger, J., Krzystek, P. and Stilla, U. (2008) ‘Analysis of full waveform LIDAR data for the classification of deciduous and coniferous trees’, *International Journal of Remote Sensing*, 29(5), pp. 1407–1431. doi: 10.1080/01431160701736448.

Reyes-Palomeque, G. *et al.* (2021) 'Mapping forest age and characterizing vegetation structure and species composition in tropical dry forests', *Ecological Indicators*, 120, pp. 106955. doi: 10.1016/j.ecolind.2020.106955.

Roberts, D.A. *et al.* (1998) 'Spectral changes with leaf aging in Amazon caatinga', *Trees - Structure and Function*, 12(6), pp. 315–325. doi:10.1007/s004680050157.

Sánchez-Azofeifa, A., Portillo-Quintero, C. and Durán, S. M. (2015) 'Structural effects of liana presence Structural effects of liana presence in secondary tropical dry forests using ground LiDAR Structural effects of liana presence', *Biogeosciences Discuss*, 12, pp. 17153–17175. doi: 10.5194/bgd-12-17153-2015.

Sánchez-Azofeifa, G. A. *et al.* (2005) 'Research priorities for neotropical dry forests', *Biotropica*, 37(4), pp. 477–485. doi: 10.1111/j.1744-7429.2005.00066.x.

Sánchez-Azofeifa, G. A. *et al.* (2017) 'Can terrestrial laser scanners (TLSs) and hemispherical photographs predict tropical dry forest succession with liana abundance?', *Biogeosciences Copernicus GmbH*, 14(4), pp. 977–988. doi: 10.5194/bg-14-977-2017.

Schneider, F. D. *et al.* (2014) 'Simulating imaging spectrometer data: 3D forest modeling based on LiDAR and in situ data', *Remote Sensing of Environment. Elsevier Inc.*, 152, pp. 235–250. doi: 10.1016/j.rse.2014.06.015.

Silva, C. A. *et al.* (2018) 'Comparison of Small- and Large-Footprint Lidar Characterization of Tropical Forest Aboveground Structure and Biomass : A Case Study From Central Gabon', *IEEE Journal of Selected Topics in Applied Earth Observations and Remote Sensing, IEEE*, 11(10), pp. 3512–3526. doi: 10.1109/JSTARS.2018.2816962.

Siyum, Z.G. (2020) 'Tropical dry forest dynamics in the context of climate change: syntheses of drivers, gaps, and management perspectives', *Ecological Processes*, 9(1).

doi:10.1186/s13717-020-00229-6.

Solberg, S. *et al.* (2017) 'Biomass and InSAR height relationship in a dense tropical forest', *Remote Sensing of Environment*. Elsevier Inc., 192, pp. 166–175. doi:

10.1016/j.rse.2017.02.010.

Stan, K. and Sanchez-Azofeifa, A. (2019) 'Tropical dry forest diversity, climatic response, and resilience in a changing climate', *Forests*, 10(5), pp. 443. doi: 10.3390/f10050443.

Sumnall, M. J. *et al.* (2016) 'Comparison of small-footprint discrete return and full waveform airborne lidar data for estimating multiple forest variables', *Remote Sensing of Environment*.

Elsevier Inc., 173, pp. 214–223. doi: 10.1016/j.rse.2015.07.027.

Vieira, D. L. M. and Scariot, A. (2006) 'Principles of natural regeneration of tropical dry forests for restoration', *Restoration Ecology*, 14(1), pp. 11–20. doi: 10.1111/j.1526-

100X.2006.00100.x.

Zhao, G. *et al.* (2021) 'Hyperspectral and Full-Waveform LiDAR Improve Mapping of Tropical Dry Forest' s Successional Stages', *Remote Sensing*, 13(19), pp. 1–27. doi:10.3390/rs13193830.